# Challenges and Accomplishments of the AIAA CFD Drag Prediction Workshop Series

John C. Vassberg[1]
*The Boeing Company, Long Beach, CA 90808, USA*

AVT-246 Progress and Challenges in Validation Testing for Computational Fluid Dynamics
Avila, Spain
26-28 September 2016

**Abstract**

**Challenges and accomplishments of the AIAA Computational Fluid Dynamics Drag Prediction Workshop (DPW) series are presented. This paper is focused on the technical aspects of the DPW series, but also includes anecdotal lessons learned while running workshops of this type. After six workshops and almost two decades in the making, this workshop series has continually assessed the state-of-the-art and state-of-the-practice of the international community's ability to accurately predict force and moment values for industry-relevant transonic aircraft configurations. From the on-set, members of the DPW Organizing Committees (OC) have always known or suspected that several key ingredients are needed for accurate CFD predictions. These include, but are not limited to: a.) grid quality, b.) grid resolution, c.) adequate turbulence modeling, and d.) solution convergence. One of our challenges has been to define metrics in each of these categories and to quantify what is required for accurate drag predictions. This is easier said than done. As it turns out, for example, grid quality seems to be an elusive metric to define. Adequacy of the turbulence model is difficult to determine for industry-relevant flows because its effect gets intertwined with many external contributing factors, including the grid, as well as the reconstruction of Reynolds stresses, to name a couple. However, quantifiable metrics for solution convergence and grid resolution have been established, but even these depend on the specific CFD method used, specific flow physics considered, and user's level of expectation for absolute and/or delta predictions. Nonetheless, progress has been made. Trends with time indicate that standard wing/body grid sizes have been increasing at a growth rate of about 20% per year while the standard deviation (scatter) of the industry's CFD results have been consistently improving. The complexity of configurations being considered throughout the industry has also been increasing with time at a rate of about 35% per year. At the highest level of CFD simulations, the state-of-the-practice is to the point now where the absolute aerodynamic performance of a well-designed transonic transport at cruise conditions can be more accurately predicted by CFD than can be measured by a build-up from wind-tunnel data with corrections to flight Reynolds numbers. These modern-day CFD predictions include the full aircraft transonic cruise configuration, trimmed to a specified center-of-gravity location, with power effects of thrust equals drag, and with real bending aero-elastic deflections. The sizes of these grid systems are well in excess of 100 million control volumes. However, accurate loads predictions over the rest of the flight envelop remain to be accomplished. Let's hope Moore's Law continues unabated for many more years to come.**

[1] Boeing Technical Fellow, AIAA Fellow, DPW Chairman

## Nomenclature

| | |
|---|---|
| Alpha | Angle of Attack |
| AR | Wing Aspect Ratio |
| b | Wing Span |
| $C_D$ | Drag Coefficient (CD_TOT) |
| $C_{DP}$ | Idealized Profile Drag = $C_D - C_L^2/\pi AR$ |
| $C_{Dpr}$ | Pressure Drag Coefficient (CD_PR) |
| $C_{Dsf}$ | Skin-Friction Drag Coefficient (CD_SF) |
| $C_L$ | Lift Coefficient |
| $C_M$ | Pitching Moment Coefficient (CM_TOT) |
| $C_P$ | Pressure Coefficient = $(P-P_\infty)/q_\infty$ |
| $C_{ref}$ | Wing Reference Chord ~ MAC |
| $C_f$ | Local Coefficient of Skin Friction |
| CFD | Computational Fluid Dynamics |
| CRM | Common Research Model |
| DPW | Drag Prediction Workshop |
| HQ | Head Quarters |
| LE | Wing Leading Edge |
| MAC | Mean Aerodynamic Chord |
| N | Number of unknowns (GRIDSIZE) |
| OC | Organizing Committee |
| RANS | Reynolds-Averaged Navier-Stokes |
| RE | Reynolds Number |
| $S_{ref}$ | Reference Area |
| SOB | Side-of-Body |
| TE | Wing Trailing Edge |
| WB | Wing/Body |
| WBH | Wing/Body/Horizontal-Tail |
| WBNP | Wing/Body/Nacelle/Pylon |
| $y^+$ | Normalized Wall Distance |
| $\alpha$ | Angle of Attack (ALPHA) |
| | Fraction of Wing Semi-Span |

## Introduction

The AIAA CFD Drag Prediction Workshop (DPW) series is a highly successful grass-roots campaign that began with hallway discussions at AIAA conferences circa 1998-1999. Several members of these hallway discussions formally established the first DPW Organizing Committee (OC) in January, 2000 with sponsorship of the AIAA Applied Aerodynamics Technical Committee. The first workshop (DPW-I) was held in Anaheim, CA during the summer of 2001, which focused on the DLR-F4 wing/body configuration due to the fact that the geometry definition and experimental data were publically available through AGARD Report 303. Unfortunately, the force and moment coefficients of these data were only published to 3 decimal places. Even by the CFD standards of 2001, this level of precision was woefully inadequate for a CFD validation database. Nonetheless, DPW-I uncovered that the level of scatter of CFD predictions throughout the international community was far greater than any of us had anticipated. Participants of DPW-I demonstrated their willingness to further contribute to this campaign by updating their results and publishing them in AIAA Papers. They also strongly encouraged the DPW Organizing Committee to continue the workshop series and plan DPW-II. This cyclic process of planning, conducting, publishing, learning, and re-evaluating the international community's desire to perpetuate the DPW Series is still on-going, with DPW-VI having been recently held in Washington DC during the summer of 2016. In addition to evolving our test cases, the DPW OCs have recognized new areas in need of CFD prediction workshops. As a consequence, we have directly spun-off members to help form and support the AIAA High-Lift Prediction Workshop and Aero-Elastic Prediction Workshop series. Furthermore, many other organizing committees have used the DPW model as the basis for their workshops, and utilize DPW OC members as consultants to help jump-start their planning efforts.

The primary goal of the DPW series is to assess the state-of-the-art/practice of modern computational fluid dynamics methods using geometries and conditions relevant to commercial aircraft. From the onset, the DPW OC has adhered to a primary set of guidelines and objectives for the DPW series. These guiding principles are:

- Assess state-of-the-art Computational Fluid Dynamics (CFD) methods as practical aerodynamic tools for the prediction of forces and moments on industry-relevant geometries, with a focus on absolute drag.
- Provide an impartial international forum for evaluating the effectiveness of CFD Navier-Stokes solvers.
- Promote balanced participation across academia, government labs, and industry.
- Use common public-domain subject geometries, simple enough to permit high-fidelity computations.
- Provide baseline grids to encourage participation and help reduce variability of CFD results.
- Openly discuss and identify areas needing additional research and development.
- Conduct rigorous statistical analyses of CFD results to establish confidence levels in predictions.
- Schedule open-forum sessions to further engage interaction among all interested parties.
- Maintain a public-domain accessible database of geometries, grids, and results.
- Document workshop findings; disseminate this information through publications and presentations.

While there have been some variations, the workshops have typically used subject geometries based on commercial transport wing/body (WB) configurations - a consensus of the OCs based on a reasonable compromise between simplicity and industry relevance. The vast majority of the participants submit results generated with Reynolds Averaged Navier-Stokes (RANS) codes, although the organizing committee does not restrict the methodology.

There are a number of reasons why the DPW workshops have been successful. It is partially due to the DPW guiding principles established by DPW-I, but it is also due to the high level of effort the participants are willing to devote to these workshops. This has no doubt been a learning experience. For example, DPW-I did not include a test case devoted to a grid convergence study, all workshops since have. We have added verification test cases based on the Turbulence Modeling Resource (TMR) website. And in DPW-V, we introduced a unified common grid family that was developed for all element types. To keep things fresh, we have varied the test cases from workshop to workshop. For example, in DPW-II and DPW-VI we included a nacelle/pylon increment, as well as asked the participants to post-process their results to measure and report the mass-flux through the flow-through nacelle. Many of the workshops request metrics quantifying the size of the SOB separation pocket. Blind test cases were included in DPW-III and DPW-IV, where the corresponding experimental data were collected after the workshops were conducted. DPW-III included a wing-body fairing increment which had attached flow with the fairing installed and separated flow at the side-of-body juncture without it; experimental data with the fairing was later made available through a collaborative effort between NASA and DLR. DPW-IV included a trimming exercise on a completely new aircraft design, the Common Research Model (CRM). DPW-VI included test cases related to grid adaption and aero-elastic effects. Needless to say, there has been a tremendous amount of time, work, budget, and luck involved to make all of this happen. New geometries have been designed, whole new wind-tunnel models have been fabricated, many wind-tunnel tests have been conducted, and the list continues; this is the list of items that most outsiders would not even think to attribute to DPW planning. A total of six DPW workshops have been conducted thus far, all in conjunction with the AIAA Applied Aerodynamics Conference for that year. For a brief description of each, see table below.

| DPW | Year | Location | Configuration | Case Descriptions |
|---|---|---|---|---|
| I | 2001 | Anaheim, CA | DLR-F4 Wing/Body | Single Point Grid Refinement Study<br>Drag Polar<br>Drag Rise Curves at Constant $C_L$* |
| II | 2003 | Orlando, FL | DLR-F6 Wing/Body<br>Wing-Body-Nacelle | Single Point Grid Refinement Study<br>Drag Polar<br>Boundary Layer Trip Study*<br>Drag Rise Curves at Constant $C_L$* |
| III | 2006 | San Francisco, CA | DLR-F6 Wing/Body w/<br>and w/o FX2B fairing,<br>W1/W2 Wing Alone | Single Point Grid Refinement Study<br>Drag Polar<br>Grid Convergence Study<br>Drag Polar |
| IV | 2009 | San Antonio, TX | Common Research Model<br>Wing/Body and Wing/Body/Tail | Grid Convergence Study<br>Downwash Study<br>Mach Sweep Study*<br>Reynolds Number Study* |
| V | 2012 | New Orleans, LA | Common Research Model<br>Wing/Body w/ Unified Grids | Grid Convergence Study<br>Buffet Study<br>Custom Grids*<br>Turbulence Modeling V&V* |
| VI | 2016 | Washington D.C. | Common Research Model<br>Wing/Body w/ and w/o Nacelle/Pylon | Grid Convergence Study<br>Nacelle-Pylon Increment<br>Aero-Elastic Effects<br>2D Airfoil V&V Case<br>Solution Adapted Grids* |

*Optional Cases

The following sections provide better overviews of the first four DPW workshops, and then the paper is completed with a detailed write-up on the fifth workshop, DPW-V.

## DPW-I, Anaheim, 2001

OK. So we were not always the finely-tuned high-performance engine that we still aren't today. When we first began this venture, none of us really knew what we were doing; at least as far as running a workshop was concerned. However, we did know how to run CFD quite well, and for several of us, our day job was to predict aerodynamic performance using RANS-based CFD methods. And while drag prediction was of utmost interest to the members of the DPW OC, we had little clue as to the level of interest others throughout the international community would have in participating in such a workshop. Our best guess was anywhere from the 10 guys on the committee to maybe 50, so we made plans for a total of 50 participants and pushed ahead. We held weekly telecons for 1.5 years before the workshop and another half-year afterwards to organize the ASM 2002 DPW sessions. Coordination with AIAA HQ proved to be a challenge initially; they wanted to view DPW as a Training Course for which they could charge each attendee $850. This was unacceptable to us, so we agreed to manage everything from DPW registration to the refreshments being served during the breaks, while AIAA provided us a room with classroom table style seating for 55 attendees. Fortunately, the AIAA APA TC provided us with a few thousand dollars of operating budget with the understanding that we might not be able to pay it back. We used this to secure refreshments and 50 custom-made leather padfolios embossed with an AIAA DPW logo. The DPW-I padfolio was a tremendous hit, and has become a collector's item. We ordered way too much food. Participants were charged $75 and attendees $125 each. We had exactly 55 people register for DPW-I, 54 showed up. We were very lucky. We reimbursed the one no-show his registration fee, and had plenty left over to repay the APA TC with a healthy return on their investment. In alphabetical order, the 10 members of the first DPW OC were: Shreekant Agrawal, Mike Hemsch, David Levy, Rick Matus, Bastian Oskam, Shahyar Pirzadeh, Juergen Quest, John Vassberg, Rich Wahls, and Tom Zickuhr.

The first Drag Prediction Workshop[1] used the DLR-F4 WB configuration due to its geometric simplicity and the availability of publically released geometry and wind tunnel results[2]. Unfortunately, the force and moment coefficients of these data were only published to 3 decimal places. Even by the CFD standards of 2001, this level of precision was woefully inadequate for a CFD validation database. In order to partially alleviate this issue, Vassberg provided a couple of techniques used to enhance data precision. But even this was unsatisfactory. The focus of DPW-I was to compare absolute drag predictions, including the variation due to grid type and turbulence model type. The results were also compared directly to the available wind tunnel data. The workshop committee provided a standard set of multiblock structured, overset, and unstructured grids for the DLR-F4 WB geometry to encourage participation in the workshop and reduce variability in the CFD results; these grids were developed using a set of gridding guidelines established by the committee. The average baseline grid size was approximately 2.5 million control volumes. Participants were also encouraged to construct their own grids using their best practices so that learned knowledge concerning grid generation and drag prediction might be shared among workshop attendees. The test cases were chosen to reflect the interests of industry and included a fixed-$C_L$ single point solution, drag polar, and constant-$C_L$ drag rise data sets. To help encourage wide participation, a formal paper documenting results was not required at the workshop. Eighteen participants submitted results of 35 data blocks, using 14 different CFD codes; many submitted multiple sets of data exercising different options in their codes, e.g., turbulence models and/or different grids. The distribution of grids was 8 multiblock, 7 unstructured, 2 overset, and 1 Cartesian. The distribution of turbulence models was 14 SA (all variants), 10 k-omega, 2 k-epsilon, and 2 others. A summary of these results was documented by the DPW-I organizing committee[3]. Because of strong participation, DPW-I successfully amassed a CFD data set suitable for statistical analysis[4]. The results of that analysis were rather disappointing, showing a 270-drag-count spread in the fixed-$C_L$ data, with a 100:1 confidence interval of more than ±50 drag counts. However, a core set of 30 data blocks were better clustered with only a 45-drag-count spread. This was still disappointing, but more along the lines of what we were expecting.

Despite the somewhat disappointing results, the consensus of the participants and organizers was that DPW-I was a definitive success. First and foremost it was initiated as a "grass roots" effort by CFD developers, researchers, and practitioners to focus on a common problem of interest to the aerospace industry. There was open and honest exchange of common practices and issues which identified areas for further research and scrutiny. The workshop framework was tested successfully on high fidelity 3D RANS methods using common geometry, grids, and test cases. Finally, it reminded the CFD community that CFD is not a fully mature discipline.

The interest generated from the workshop was continued and resulted in several individual efforts documenting results more formally[5-8], presented at a special session of the 2002 AIAA Aerospace Sciences Meeting and Exhibit in Reno, NV. The interest generated by DPW-I naturally led to the planning and organization of the second AIAA Drag Prediction Workshop, DPW-II. The DPW-II organizing committee, recognizing the success of DPW-I, maintained the format and objectives for DPW-II.

## DPW-II, Orlando, 2003

Having learned a lesson or two from the first workshop, we knew that registration and refreshments were a pain for us to manage. We worked with AIAA HQ to get them to handle DPW registration and refreshments, to provide DPW padfolios, to provide a meeting room over the weekend to hold the workshop, and to keep the registration fees down to $200 or less. The business case that we argued was that the DPW workshops were bringing in additional conference attendees; they are coming because of the workshop and then staying for the conference, and would have otherwise not come. Further, we were providing our services free of charge, so the only real expense AIAA HQ had to cover was that of the refreshments and padfolios. As a consequence, AIAA HQ justified this additional burden on their part. This left us with the ability to focus on the technical aspects of running a workshop. Believe it or not, this was a major accomplishment for the DPW OC, and one that all other AIAA workshops have inherited without knowing the history. The attendance of DPW-II was a little over 80, but a few may have snuck in the back while the AIAA staff was not watching. The room that AIAA reserved for us was large enough to seat about 100. However, there were two issues with it that compounded to make matters very unfavorable for anyone sitting more than two or three rows back. First, the ceiling was only about 7 feet high, which limited the height of our projection screen. Second, the room was fairly narrow, which limited the number of people sitting abreast and required many rows of seating. Attendees sitting in the back simply could not see the screen at all. But we live and learn. Another aspect of the DPW OC that we wanted to achieve was some level of turn-over in membership, striking a balance between old and new blood. Between I and II, we experienced a 70% turnover rate, which was more than we had hoped. Those that retired, cited the significant amount of work required. Fortunately, those that signed up were less informed. Those that stayed, should have known better. The 10 members of the DPW-II OC were: Olaf Brodersen, Jean-Luc Godard, Steve Klausmeyer, Kelly Laflin, Joe Morrison, Mark Rakowitz, Ed Tinoco, John Vassberg, Rich Wahls, and Tom Zickuhr.

The second workshop[9] used the DLR-F6 wing/body (WB) and wing/body/nacelle/pylon (WBNP) geometries. A set of baseline grids were provided by the OC, based on a refined set of gridding guidelines. The average WB grid size for the practice-of-the-day was about 4.8 million control volumes. The maximum WB and WBNP grid sizes were 10.0 million and 13.7 million control volumes, respectively. The DPW-II OC worked with DLR and ONERA to make pertinent experimental data available to the public domain. One specific objective of DPW-II was the prediction of the incremental drag associated with nacelle/pylon installation. Another objective was to include a grid resolution study. The scatter for the WB data was about 26 drag counts, and about 42 counts for the WBNP configuration. The incremental drag due to NP was computed to be about 60-63 counts, whereas the experimental data showed only a 43 count delta. Even the predicted NP delta did not come close to the experimental measurements. This finding was definitely a contradiction to the industry's assumption that accurate drag increments could be predicted with CFD. The F6 geometry contained pockets of flow separation more severe than the F4; occurring predominantly at the wing-body and wing-pylon juncture regions.

Results from the workshop were documented with a summary paper,[10] a statistical analysis,[11] an invited reflections paper[12] on the workshop series, and numerous participant papers[13-21] in two special sessions of the 2004 AIAA Aerospace Sciences Meeting in Reno, NV. Of particular note is the work by Yamamoto, et al.[20] This work showed a dramatic improvement for the simulation of separated juncture flows using an implementation of a Quadratic Constitutive Relation (QCR) for turbulent stresses. QCR quickly became the standard for accurate juncture-flow simulations, and is considered one of the more significant accomplishments prompted by the DPW series. A conclusion of DPW-II was that the separated flow regions made it difficult to draw meaningful conclusions with respect to grid convergence and drag prediction. During the follow-up open-forum discussions, the CFD community voiced the desire for the organizing committee to include in the third workshop: a) blind test cases, b) simpler geometries, and c) a fixed-alpha grid resolution study. The request for blind test cases is motivated by an earnest attempt to better establish a measure of the CFD community's capability to predict absolute drag, rather than match it after-the-fact. The request for simpler geometries allows more extensive research in studies of asymptotic grid convergence. The request for a fixed-alpha grid-resolution study was prompted by the need to understand why fixed-lift is so important during drag prediction.

**DPW-III, San Francisco, 2006**

Just when we thought we almost knew what we were doing, and AIAA convinced of it, along came DPW-III. We were pleased that DPW attendance experienced some growth between DPW-I and DPW-II. However, and without consulting with us, the AIAA staff counted on this growth to continue in exponential form. Since there was a 50% growth between DPW-I and II, they anticipated the same growth from DPW-II to III, thus needing accommodations for 125 attendees for DPW-III. We were hoping for 70 to show up, as the venue was too attractive for any reasonable person to stay indoors on a weekend for a technical workshop. AIAA provided a huge theater room with copious seating capacity. The final attendance of DPW-III was about 65, and needless to say, we had plenty of padfolios and refreshments to go around. The OC turnover rate between II and III was a manageable 30%, with just enough new blood to provide fresh ideas. The 10 members of the DPW-III OC were: Olaf Brodersen, Bernhard Eisfeld, Kelly Laflin, Mori Mani, Dimitri Mavriplis, Joe Morrison, Ed Tinoco, John Vassberg, Rich Wahls, and Tom Zickuhr.

The third DPW workshop[22] retained the DLR-F6 WB as the baseline configuration to provide a bridge to the previous workshop. However, to test the hypothesis that the grid-convergence issues of DPW-II were the direct result of the large pockets of flow separation, a new wing-body fairing was designed to eliminate the side-of-body separation. Details of the FX2B fairing design are documented by Vassberg[23]. To help reduce the wing upper-surface trailing-edge flow separation, a test case at higher Reynolds number was introduced. Changes in both geometry and flow condition also provided the DPW-III participants a blind test since no test data (specific to these cases) would be available prior to the workshop. A total of 70 grids were provided by 12 organizations about the two F6 WB configurations in a 3-member family of coarse, medium, and fine levels. The nominal sizes of these grids were 2.7, 8.0, and 24 million control volumes, respectively. The average WB medium mesh size was 8.5 million. Fifteen participants submitted a total of 26 data blocks for the FX2B fairing test cases. Unanimously, all of the participants detected absolutely no SOB separation with the FX2B fairing installed. The scatter for the F6 (with SOB separation) was about 16 counts, while that for the FX2B was about 20 counts. However, the standard deviations of these results were 6.0 counts and 4.9 counts, respectively. Hence, these findings neither confirm nor deny the hypothesis that flow separation is a dominant source of scatter in CFD simulations. Reflecting on the scatter of DPW-II (albeit at a different Reynolds number), the scatter for the F6 WB is much improved in DPW-III over the results from DPW-II. Could this be due to size of grid or less participation or better execution of CFD or all of the above? Yes, it could be, but we are still not sure how these and other factors may interplay.

For a completely different set of test cases, two wing-alone geometries were created to provide workshop participants with simpler configurations on which more extensive grid-convergence studies could be conducted; these wings were designed to exhibit no appreciable separation at their design conditions. In a similar manner as for the WB cases, a total of 30 wing-alone grids were provided by 5 organizations, about both wings, at three grid-resolution levels. Eleven participants provided 11 data blocks for the wing-only test cases. The fixed-alpha grid-resolution study showed a scatter in lift of about 14%, and in drag of about 32 counts. Even a simple correction for lift reduces the scatter in drag (idealized profile) to about 9 counts for these wing-alone cases. An accomplishment of DPW-III was that the community at large was enlighten to the fact that absolute drag about winged configurations is a direct function of lift, and only an indirect function of alpha.

DPW-III was heavily documented with summary papers[24,25], a statistical analysis paper[26], participant papers[27-30], and a special section of the AIAA Journal of Aircraft, edited by Vassberg[31–36]. After three workshops, the organizing committee recognized that a recurring theme of the workshop series was related to grid quality and resolution; see Mavriplis, et al.[37]. On the other hand, the following quote can be found in the DPW-III summary paper. *"A general observation, after reviewing all the results, is that there is a set of CFD codes whose members all seem to agree relatively well with each other, and do so over all of the test cases spanning the DPW series. Most noteworthy about this core set of codes is that it is comprised of flow solvers that are based on all types of grids. Hence, several unstructured and hybrid mesh solvers have matured sufficiently to be useful CFD tools for accurate drag predictions. Alternatively, a solver based on structured meshes does not automatically imply the same."* Hence, progress had been made by 2006, but much more is needed yet, even a decade later.

## DPW-IV, San Antonio, 2009

It seems like every venue has thrown a monkey wrench into the gears, and DPW-IV was no different. There were 59 registered attendees for DPW-IV. Yet when we showed up the day before the workshop, the room assigned to us could only hold about 30 people. Fortunately, AIAA staff also recognized this issue and managed to locate a room within the hotel that could accommodate 70 in a classroom style table seating arrangement. Problem averted. The temperature outdoors hit 113º later that week, but the atmosphere along the River Walk was comfortable and provided many restaurants within a short distance to select from. The OC turnover rate between III and IV was 20%, but one of the "new" guys was actually an old guy returning from DPW-I. The 10 members of the DPW-IV OC were: Olaf Brodersen, David Levy, Mori Mani, Dimitri Mavriplis, Joe Morrison, Mitsuhiro Murayama, Ed Tinoco, John Vassberg, Rich Wahls, and Tom Zickuhr.

For the fourth DPW workshop[38] a completely new aerodynamic design was developed by Vassberg, et al.[39]. This wing/body/horizontal-tail/nacelle/pylon configuration is representative of a contemporary high-performance transonic transport, whether the nacelle/pylon group is installed or not. This configuration is referred to as the Common Research Model (CRM). The concept of the CRM was formulated through a collaborative effort between NASA's Subsonic Fixed Wing (SFW) Aerodynamics Technical Working Group (TWG) and the DPW Organizing Committee. NASA agreed to build and test the CRM in their facilities, as well as to loan it out to other wind tunnel facilities as requested. Another aspect of DPW-IV different from the first three workshops was in the timing of the availability of wind-tunnel test data on the subject geometries. In DPW-IV, the workshop was held before any experimental data were collected and therefore provided a true set of blind test cases. Another advantageous outcome of this collaborative endeavor is that the CRM has now been tested in multiple facilities thus far, and much of the data from these tests are publicly available. The National Transonic Facility (NTF) at NASA Langley tested the CRM during Jan-Feb 2010, and then it was evaluated at the Ames 11-ft wind-tunnel during Mar-Apr 2010. Data from the NTF and Ames tests have been released to the public domain by Rivers and Dittberner[40-42]. In addition, the CRM has been tested in the ETW, and JAXA and ONERA have each developed their own versions of the CRM which they have tested in their facilities, respectively. Some of these data can also be downloaded from the CRM website maintained by Rivers[42]. Due to past observations of grid dependence on solutions, a greater emphasis was placed on establishing a comprehensive set of meshing guidelines for the generation of baseline grid families. With these guidelines in place, grids were requested from several organizations for structured multiblock, overset, and unstructured types. Each grid family was required to include a Coarse (C), Medium (M), and Fine (F) grid; adding an optional Extra-Fine (X) grid was also encouraged. Target sizes for these grids were 3.5, 10, 35, and 100 million control volumes, respectively. The Medium mesh was intended to be representative of current engineering applications of CFD being used to estimate absolute drag levels on similar configurations. A total of 74 meshes of 18 families were provided and made available. The fourth workshop requested grid convergence and Mach sweep computations as in the previous workshops, plus downwash and Reynolds Number studies. Data were submitted from 19 organizations totaling 29 individual datasets. For the grid refinement study, a Richardson Extrapolation methodology was employed to estimate a continuum value for the total drag coefficient. The range for the total drag coefficient spanned 152 counts. (Excluding a single outlier, the scatter band for DPW-IV reduces dramatically to 41 counts.) This is a definite improvement since DPW-I, and although it is quite significant, the confidence level is still not down to a low enough level to compete with experimental methods. Despite the emphasis placed on grid generation with the intent of reducing the associated errors, the variation in the DPW-IV results was still somewhat disappointing.

Documentation for the DPW-IV results can be found in summary papers[43-44] and in individual contributing papers[45-58] from two special sessions held at the 28th Applied Aerodynamics Conference in June 2010. Of particular note, Sclafani, Vassberg and Pullium[45] collaborated to extend their overset grid family to 2.4 billion nodes. This proved to be a significant challenge, as practically every step in the numerical simulation process seemed to break with the extreme grid sizes involved. For example, even the unformatted plot3d files could not accommodate grid blocks in excess of ~33 million nodes. To address this single issue, the basic 17-zone overset grid system was split into an 81-zone grid system at the extra-fine mesh level with 213 million grid points. This grid was then refined to develop a 714 million node super-fine grid and a 2.4 billion node ultra-fine grid. The multitude of issues was finally resolved after about three months of effort of fixes. The resulting grid-convergence trend-line of the extreme grid family was consistent with the trend-line previously established by the coarse, medium, fine and extra-fine grid sequence. This accomplishment verified that the baseline DPW-IV overset grid family is definitely well within the asymptotic range for OVERFLOW and gives hope that the remaining baseline grid families fall well within the asymptotic range too. This exercise also provided us the ability to maintain uninterrupted OVERFLOW solutions for over a decade of growth for our biggest grid systems; a very nice side benefit of participating in the DPW series.

## DPW-V, New Orleans, 2012

Just when we conditioned ourselves to expect the unexpected, the unexpected happened – there was absolutely nothing wrong with the venue at New Orleans. In fact, it was an amazing room, perfectly sized and configured. The AIAA staff had secured the Art Gallery in the hotel for DPW-V. On display was a collection of original Blue Dog paintings by George Rodrigue. Life was good in the Big Easy. The OC turnover rate between IV and V was 25%. The 12 members of the DPW-V OC were: Olaf Brodersen, Simone Crippa, Kelly Laflin, David Levy, Mori Mani, Dimitri Mavriplis, Joe Morrison, Mitsuhiro Murayama, Ben Rider, Ed Tinoco, John Vassberg, and Rich Wahls.

For the fifth workshop[59], the test cases focused on force and moment predictions for the CRM wing/body configuration, including a grid refinement study and an optional buffet study. However, a new approach to our baseline grids was taken; the goal being to reduce grid-related scatter in the data. We have always recognized that maintaining continuity across baseline grids was an essential element to compare CFD results across all flow-solver types, yet also knew this would be a severe challenge. This was usually handled by publishing a set of gridding guidelines for generation of the baseline grids; these guidelines were used by the various developers of the various types of baseline grids. However, this approach has only been partially successful. Each grid developer would adhere to these guidelines mostly, but would deviate from them if it would reduce their effort for grid generation. Furthermore, it is nearly impossible to ensure a true parametric family of unstructured meshes with this approach. Addressing this fundamental issue was the foundation of DPW-V. Here, a high-quality high-resolution multiblock structured mesh was generated, and then this was used to derive a unified common grid sequence. Six levels of refinement were created resulting in grids ranging from $0.64 \times 10^6$ to $138 \times 10^6$ hexahedra, spanning more than 2.3 orders-of-magnitude in size. Then overset and unstructured grids were derived, maintaining the cloud of grid nodes as well as the volumetric discretization down to the hexahedral level. The overset grid used extra zones comprised of point-matched bridging grids at internal block-interfaces to couple the neighboring zones. The unstructured grids were defined in hexahedral, prismatic, and tetrahedral elements. A hybrid grid with prismatic boundary layer and tetrahedral field elements was also defined. Here, each hexahedron was broken into two prisms, and then, each prism was decomposed into three tetrahedra. This unique collection of grids was designed to substantially remove the effects of grid variation on the computed results. Further, the families of unstructured meshes were now truly parametric in local cell sizes as well as local connectivity. DPW-V studies showed reduced scatter and standard deviation from previous workshops. This reduction in scatter supports the fact that grid quality and grid resolution matter. However, since scatter still exists in the DPW-V data, other factors such as turbulence modeling, code bugs, boundary conditions, up-winding, etc. can matter as well.

The test cases included a grid refinement study using the unified common baseline grids and/or user-supplied custom grids if desired. The second case focused on buffet prediction with a finely spaced alpha sweep spanning the range where flow separation on the wing was observed in the wind tunnel data. This was a change from DPW-IV, where angle-of-attack sweeps from 0 to 4° were calculated for the purpose of determining trimmed drag polars. For a commercial transport like the CRM, high-speed lines development is very important as it determines whether or not speed and range goals are met. Significant effort must also be paid to loads, handling qualities, and other constraints which are required to meet structural and certification requirements. Many of these high-speed flight concerns occur at the edges of the flight envelope, which are characterized by large regions of separated flows. For the fifth Drag Prediction Workshop the buffet study has been included to assess CFD prediction in this regime. The optional third test case used geometries, grids, and conditions from the Turbulence Model Resource (TMR) website[61] prepared by the Turbulence Model Benchmarking Working Group. Three sub-cases were included in DPW-V: 1) 2D Zero Pressure Gradient Flat Plate, 2) 2D Bump-in-Channel, and 3) 2D NACA 0012 Airfoil. These test cases were designed to discriminate between turbulence model implementations through rigorous grid convergence studies.

Documentation for the DPW-V results can be found in summary papers[64-65] and in individual contributing papers[66-71] from a special session held at the 51st Aerospace Sciences Meeting in January 2013. These papers and others from DPW-IV in 2014 were featured in a special edition of the AIAA Journal of Aircraft devoted to the Drag Prediction Workshop[72], edited by Vassberg and Lee-Rausch.

The remainder of this paper presents a detailed review of the geometry and grid definitions used for the DPW-V, with a focus on the Case 1 grid-refinement study based on the unified baseline grid family. Participant data are presented, including force and moment predictions, wing pressure distributions, and flow separation at the wing/body trailing edge juncture. A Richardson extrapolation is performed to estimate the continuum force levels. Although not necessarily applicable, comparisons to force, moment, and pressure data from the NTF and Ames wind tunnel tests have been included for reference.

## DPW-V Geometry – NASA CRM Wing/Body

The subject geometry for DPW-V Cases 1 and 2 is the Common Research Model[39] (CRM) developed jointly by NASA's Subsonic Fixed Wing (SFW) Aerodynamics Technical Working Group (TWG) and the DPW Organizing Committee. The CRM represents a modern transonic commercial transport airplane, and was designed in the full configuration with a low wing, fuselage, horizontal tail, and engine nacelle/pylons mounted below the wing. However, for this workshop, only the wing/body configuration was used. A rendering of the WB geometry is shown in

Figure **1**, along with a photo of the wind tunnel model installed in the NASA Ames 11ft Transonic Wind Tunnel (with horizontal tail). The CRM was also the subject geometry for DPW-IV.

The wing is designed for a nominal conditions of Mach=0.85, $C_L$=0.50, and Reynolds number $43x10^6$ based on $C_{ref}$. Pertinent geometric parameters are listed in Table 1. The Boeing Company developed the aerodynamic design of the CRM, which includes a supercritical wing. Certain features are designed in to the wing profile for the purposes of research and development. For example, the upper-surface pressure recovery over the outboard wing is intentionally made aggressively adverse over the last 10-15% local chord. This promotes separation of the upper-surface boundary layer in close proximity to the wing trailing edge (TE) at lifting conditions at and above the design point. The relatively strong adverse pressure gradient amplifies the differences in various turbulence models that were employed by DPW participants. Another feature is that the span loading was designed to be very nearly elliptical as compared to a more practical design which would use a compromise distribution (more triangular) to reduce structural loads and decrease airframe weight. This feature is included to provide a challenge for possible future workshops on aerodynamic shape optimization which might explore structure and fuel weight trade-offs. The wing-body fairing design provides fully-attached juncture flow at flight Reynolds number, but not necessarily so at wind-tunnel conditions.

## DPW-V Unified Common Grid Family

As mentioned before, a common theme and discussion topic in the DPW series has been the effect of the computational grid on the results. Previously, a substantial effort was made in DPW-IV to address this, yet there was still significant variation in the results among the different grid types. The Organizing Committee recognized that a relatively simple Multiblock Structured (MB) grid could be created for the CRM wing/body geometry that conformed to the desired gridding guidelines. These gridding guidelines have been developed over the course of the DPW series and are listed in Table 2. The grid topology for the MB grid is shown in Figure 2. Although the topology of the MB grid is relatively simple, the generation of a high-quality high-resolution mesh which conformed to the gridding guidelines was not a trivial task.

The finest grid (L6) was generated first and sized to extend well into the asymptotic range of grid convergence, while the coarsest grid (L1) would still be "multigrid friendly" for up to 3 levels. The next coarser level (L5) was obtained from L6 by replacing every three cells in each of the I, J, & K directions with two cells. The L4 and L3 grids were created from L6 and L5 by removing every other point in each of the I, J, & K directions, respectively. The process was repeated with the L4 and L3 grids to complete the sequence at L2 and L1. By interleaving the even/odd levels, a complete family of six grids was constructed with "4-3-2" parametric variation. For more information regarding the generation of the unified grid system, see Vassberg[60].

Once the MB series was developed, then a set of unified grids for other types were derived. The Overset series used data from neighboring blocks to define patch grids to bridge each block; a total of four bridge grid zones were created. The patch grids overlap each block by three cells as shown in Figure 3, and are point matched to annihilate interpolation errors with the exception of one issue on the K=1 plane for the mid-body block, where the singular J line has mixed symmetry plane and block boundary conditions.

Three types of unstructured grids were created from the MB grids: hexahedral, prismatic, and hybrid (prismatic in the boundary layer and tetrahedral in the field). The hexahedral format preserves the structure of each individual cell of the MB grids, but converts the file into finite element form with no IJK structure. Subdivision of hexahedral elements into prismatic and tetrahedral elements follows the sequence shown in Figure 4a. Each hex cell subdivides into 2 prism cells, and then each prism is split into 3 tetrahedra. A fully tetrahedral grid could not be created due to issues at the trailing edge of the wing. Groups of cells inside the boundary layer grid were distorted such that a negative volume would result when subdivided into tetrahedra (Figure 4b). Since this issue was confined to a very local region well within the boundary layer, a hybrid grid family could be created with prisms in the boundary layer and tetrahedral in the outer flowfield.

A summary comparison of the grid sizes for all levels and types is listed in Table 3. Note that suitable grid refinement sequences are available for unstructured cell- or node-based schemes.

## DPW-V Test Cases

It is recognized that many of the DPW participants may have limited time and/or resources to devote to this type of study. The test case specifications, as with the grid definitions, are set to encourage participation by restricting the number of cases to a manageable number while also providing a challenge to test the state of the art/practice in CFD prediction capabilities. While this paper is focused on Case 1, for completeness, all test cases are described. These contain a set of required and optional conditions:

**Case 1 – NASA Common Research Model (CRM) Wing/Body Common Grid Study:**

1. (Required) Grid Convergence study at Mach = 0.85, $C_L = 0.500$ (±0.001)
   - Grid refinement using the unified common grid sequence consisting of at least four grid levels
     - Target grids should range from 3 to 50 million control volumes
   - Chord Reynolds Number RE = $5x10^6$ based on $C_{ref} = 275.80$ in
   - Reference Temperature = 100° F
   - Moment reference center is $x_{ref} = 1325.90$ in, $z_{ref} = 177.95$ in
2. (Optional) – Grid Convergence study using participant developed grids:
   - All participants are encouraged to build their own grids using 'best practice' techniques

**Case 2 – (Required) – NASA Common Research Model (CRM) Wing/Body Buffet Study:**

- Mach = 0.85
- Drag Polar for alpha = 2.50°, 2.75°, 3.00°, 3.25°, 3.50°, 3.75°, 4.00°
- Medium Grid used in Case 1 from the Common Grid Sequence or participant developed grids
- Chord Reynolds Number RE = $5x10^6$ based on $C_{ref} = 275.80$ in
- Reference Temperature = 100° F

**Case 3 – (Optional) – Turbulence Model Verification:**

1. 2D Zero Pressure Gradient Flat Plate: $M = 0.20$; $RE_L = 5x10^6$; $T_{ref} = 540°$ R
2. 2D Bump-in-channel: $M = 0.20$; $RE_L = 3x10^6$; $T_{ref} = 540°$ R
3. 2D NACA 0012 Airfoil: $M = 0.15$; $RE_C = 6x10^6$; $T_{ref} = 540°$ R

All CRM simulations are to be "free air" with no wind tunnel walls or support system. The boundary layer is to be modeled as "fully turbulent" for all cases. No free or fixed laminar-to-turbulent transition is to be specified. To collect a consistent set of data from each participant, template datasets are supplied. These templates request lift, drag (broken down into skin friction and pressure components), pitching moment, pressure distributions at specified span stations, trailing-edge separation locations, dimensions of the side-of-body separation bubble, grid family and sizes, turbulence model, computing platform and code performance, number of processors used, number of iterations required, etc. These workshops capture an extensive amount of information that serve as a snapshot of the industry capabilities of the time. For example, in the four workshops held thus far, one obvious trend is that the grid size has grown dramatically. The average size of the medium WB meshes in DPW-I through DPW-IV have been 2.5, 4.8, 8.5 and 10.9 million, respectively. This represents a growth rate of ~20% per year during the eight years between DPW-I and DPW-IV. For DPW-V, the definition of its "Medium" mesh did not have the same relevance to industry norms as in the previous workshops. However, the finest-level grids from the DPW series have increased steadily over the years, starting with about 13.7 million control volumes in DPW-II to 138 million in DPW-V, showing a growth rate of ~35% per year. This growth rate is indicative of how fast CFD simulations are increasing throughout the industry. It is comprised of growth in grid size for a given problem and compounded with growth in geometric complexity of the problems being analyzed. In addition to this expansion in grid sizes, the complexity of flow physics being simulated and number of cases run are also increasing. At the highest level of CFD simulations, the state-of-the-practice is to the point now where the absolute aerodynamic performance of a well-designed transonic transport at cruise conditions can be more accurately predicted by CFD than can be measured by a build-up from wind-tunnel data with corrections to flight Reynolds numbers. These modern-day CFD predictions include the full aircraft transonic cruise configuration, trimmed to a specified center-of-gravity location, with power effects of thrust equals drag, and with real bending aero-elastic deflections. The sizes of these grid systems are well in excess of 100 million control volumes. However, what we have left to accomplish are accurate loads predictions over the rest of the full flight envelop. Let's hope Moore's Law continues unabated for many more years to come.

## DPW-V Participation

Drag Prediction Workshops are open to any individual, group or organization wishing to perform the calculations according to the specifications set out by the organizing committee. Response for DPW-V followed the trend of gradually increasing participation over the DPW series. The level of participation in DPW-V was excellent by many counts. Users submitted data from a wide variety of sources, code types, grid types, and turbulence models. Many performed studies which specifically addressed the effects of gridding and/or turbulence modeling with the same code. As mentioned above, the geometry, test cases, and data format were all uniformly controlled to facilitate the analysis. A total of 57 datasets were submitted from 22 different teams or organizations. The demographics of these teams are broken down by location and type as follows:

- 10 North America, 5 Europe, 6 Asia, 1 South America
- 9 Government, 5 Industry, 6 Academia, 2 Commercial

Grid type and turbulence model breakdown are:

- **Grid Types:**
  - 5 Unified Common Overset (4 Teams)
  - 7 Unified Common Structured Multiblock (5 Teams)
  - 25 Unified Common Unstructured (13 Teams: 14 Hex, 7 Hybrid, 4 Prism)
  - 20 Custom User Generated (7 Teams: 6 Overset, 2 MB, 2 Hex, 8 Hybrid, 2 Tet)
- **Turbulence Models:**
  - 38 SA (all types)
  - 13 SST (all types)
  - 4 Goldberg $R_T$
  - 1 EARSM
  - 1 Lag-RST

All participants were asked to submit force/moment, pressure, and separation data in the standard format. The large number of datasets poses a challenge in the presentation of the data. Each dataset is assigned an alphanumeric (including Greek) symbol while colors and line types are used to denote grid or turbulence model type depending on context. All of the force, moment and pressure plots follow the scheme listed in Table 4.

## DPW-V Case-1 Results: CRM at Cruise Mach and Lift

The first test case is focused on the grid refinement study for the CRM Wing/Body at M=0.85 and $C_L$=0.500. Trends with grid size for total drag are shown in Figure 5, broken out by grid type and turbulence model. Overall, the scatterband reduces considerably as the grid is refined, and the bulk of results converge to a band about 10-15 counts wide. There is no clear advantage of any one grid type in terms of a reduced scatter. With one exception, similar trends can be observed for the turbulence models. The Goldberg $R_T$ model (Datasets M, O, Q, and S) clearly predicts the drag to be higher, although some of the SST results (T and P) with the same code are high as well. The two other sets from this team (N and P) which use the SST model compare well with the other SST results. Most of the SST results have a shallower trend with grid size and agree with each other very well even though they represent the results of six different codes and multiple grid types. Similar trends are seen in the skin friction and pressure drag components, see Figure 6 and Figure 7, respectively. The skin friction does not vary significantly with grid resolution, confirming that grid refinement beyond a certain level (e.g., $y^+$ ~1) is not needed to resolve the boundary layer for most of the grids and turbulence models. This conclusion likely does not apply to larger regions of separation or to wakes. Alpha and pitching moment for $C_L$=0.500 are shown in Figure 8. Other than a few outliers, the trends are very flat with grid size. Alpha falls generally in the range from 2.1°-2.3°, and the spread in pitching moment is ~0.02. For typical tail configurations, the latter represents a stabilizer incidence range of about 0.5°. When plotted on scales that show all data, it is difficult to glean out detailed trends. Expanded scaled plots are shown in Figure 9, with scales chosen to highlight the bulk of the data. Specific datasets are easier to identify, and nonlinear grid convergence trends become more apparent. No particular effects due to grid type are observed.

A standard technique in grid convergence studies is to use Richardson extrapolation. As implemented here, a standard least squares quadratic curve fit is used with grid factor, $N^{-2/3}$, where N is the number of control volumes. For second order codes the fit should reduce to linear with decreasing error as long as the refinement is in the asymptotic range. The y-intercept estimates the theoretical infinite resolution (continuum) result. Extrapolations are shown in Figure 10.

Also shown here are wind tunnel results from the NASA NTF and Ames tests, which warrants some discussion. Differences in the "test" set-up between Wind Tunnel and CFD are well known, and a few are listed below:

| Wind Tunnel | CFD |
|---|---|
| Walls | Free Air |
| Support System (Sting) | Free Air |
| Laminar/Turbulent (Tripped) | "Fully" Turbulent (usually) |
| Aeroelastic Deformation | Rigid 1G Shape |
| Measurement Uncertainty | Numerical Uncertainty and Error |
| Corrections for known effects | No Corrections |

Clearly there are potentially significant differences between what Wind Tunnel and CFD are measuring/computing. It is important to assess differences in magnitude between wind tunnel and CFD, but until the above variables are better addressed we should consider that the wind tunnel data are included here for reference only.

As described above, the common grid study is a key feature of DPW-V. Figure 10a shows total drag coefficient results for all submissions, while Figure 10b shows only the Common Grids which use the exact same node distributions. A quite significant variation in the solutions remains, which may be due to the cell subdivisions into prisms and tetrahedra. So the data are further reduced to only hex-based grids – Structured, Unstructured, and Overset – in Figure 10c. Any remaining variation must be due to specifics of the CFD method coding, including turbulence model.

Figure 11a shows the angle of attack for $C_L$=0.500, while Figure 11b shows the pitching moment. All the methods predict alpha to be too low compared to the wind tunnel – a result that has been present in all previous workshops. Part of the reason for this is wing aeroelastic bending, but it is likely not the entire reason. Pitching moment is also too negative, also at least partly from wing bending.

The continuum drag estimates are shown in Figure 12. Average and median $C_D$ are 0.02516 and 0.02496, respectively. The spread in the drag coefficient is 27.9 counts, while the standard deviation is 5.3 counts. These represent a small but definite improvement from DPW-IV, which were 40.9 and 8.1 counts, respectively. However, upon closer inspection of the data, six of the eight data outside the standard deviation are from the same Participant. If these six data blocks are omitted, then the standard deviation drops to 3.4 counts, and this represents a significant improvement over DPW-IV. The median solution is about 4 counts higher than the averaged wind tunnel data. The difference between the NTF and Ames data is about 8 counts, similar to the standard deviation of the CFD data. As mentioned above, we should expect differences between wind tunnel and CFD results due to the differences in "test" set-up. Although the exact magnitude of these differences is not known, it is still a good sign that the data agree reasonably well.

Pressure coefficients at six stations along the wing span are shown in Figure 13 for the Level 3 grid submissions. The level of scatter and agreement with wind tunnel data are generally very good although both tend to deteriorate as the span station progresses to the wing tip. The tunnel data for the outboard stations tend to have lower leading edge suction peaks than the CFD results. This trend may be the result of aeroelastic deformation of the wing on the wind tunnel model, which would lower the tip incidence on a swept wing. Effects of grid refinement are shown in Figure 14 for Station 10 ($\eta$=.5024). Note that fewer pressure datasets were provided for Levels 1, 5, and 6, and that should be taken into account as it magnifies the decrease in scatterband at higher grid resolutions. There is no fundamental change in shock location with the finer grids. There are no observable trends with grid type or turbulence model in the pressure distributions. (The data for entry "k" is as submitted; there is no explanation for the apparent shift in pressure.)

## DPW-V Conclusions

The fifth AIAA CFD Drag Prediction Workshop was held in conjunction with the 30th AIAA Applied Aerodynamics conference in June, 2012. The event was well attended by a diverse group of expert CFD practitioners from four continents representing government, industry, academia, and commercial code development institutions. This workshop focused on a common grid study for the NASA Common Research Model wing/body configuration, including single point grid convergence and high-alpha buffet conditions. An optional turbulence model verification study was also included.

A total of 57 Reynolds Average Navier Stokes datasets were provided on structured, overset, and unstructured grids. Of these, 37 used unified common grids all derived from the identical field of points regardless of grid type. For the Case 1 grid convergence study, a Richardson extrapolation was performed to estimate continuum results. Total scatter and standard deviation were reduced from DPW-IV. Comparison of the results to wind tunnel data is reasonable, within about 4 counts to the median solution. However, since the wind tunnel test and CFD problem

setups are inherently different, there is some question as to how well they *should* agree. There are no clear breakouts with grid type or turbulence model, with the exception of the Goldberg $R_T$ model which predicted higher drag than the bulk of the other solutions – especially for the coarser grids.

## DPW Series Historical Trends

After six workshops spanning almost two decades, the DPW Series has generated a tremendous amount of CFD data, freely available to the public domain. From these data, a set of historical trends are presented. For example, Figure 15 illustrates how the scatter of drag prediction for the DPW Wing/Body Cases has improved over the course of the DPW Series. Here, the scatter bands are given for all data submitted and with outlier data omitted. Figure 16 provides this same trend without the outlier data. In general, note that the scatter has shown progressive improvement over the years with an apparent exception for DPW-IV. The reason for this increase in DPW-IV is due to the fact that this test case included a horizontal-tail and an associated trimming exercise. The extra complexity of the test case certainly influenced the participants' ability to predict drag at a trimmed condition.

During the DPW Series, we have interjected various types of complexities into the test cases. For example, in DPW-II, we added geometric complexity by adding a Nacelle/Pylon group to the Wing/Body configuration. Again, additional complexity in the test cases increased the scatter of the drag as depicted in Figure 17. Here, the WB scatter of predicted drag was about 26 counts, whereas for the WBNP configuration it jumped to about 42 counts. In DPW-II, we also asked the participants to provide a delta-drag estimate of the Nacelle/Pylon group. At the time, the CFD community felt that while absolute drag levels might be difficult to predict, delta-drag increments could be accurately assessed. Interestingly, the NP delta-drag computed in DPW-II was about 60-63 counts, while experimental wind-tunnel test measured an NP delta of only 43 counts, see Figure 18. Maybe we were not so well off after all with incremental predictions. In particular, this test case was made difficult for accurate drag predictions by juncture-flow separations at both the wing-body intersection and the pylon-wing intersection lines. The recurring theme of juncture-flow separations causing difficulties with CFD drag predictions has been the motivation for an on-going effort to develop a Juncture-Flow Model (JFM). The JFM campaign will gather off-body data in juncture-flow regions for attached flows, flows at incipient separation, and flows with moderately sized separation bubbles. The intent for these measurements is to provide the turbulence modeling community with high-quality, high-resolution databases to help advance the next generation turbulence models.

Although it has been difficult separating out the parts and pieces that contribute to errors in CFD drag predictions, much of the improvements over the years can be attributed to grid resolution. Figure 19 illustrates the growth in grid sizes during the DPW Series. For DPWs I-to-IV, we consistently included a test case that asked participants to include a "Medium" Wing/Body grid that represented the current state-of-the-practice for accurate drag predictions. This growth is provided by the blue bars of Figure 19, shown on a semi-log scale. When holding geometric complexity constant, the grids have been growing in size by about 20% per year since 2001. The DPW Series has also included various forms of geometric complexity and increased grid-convergence requirements. The maximum grid sizes of the structured meshes for DPWs II-to-V are provided by the red bars of Figure 19. Note that this growth is about 35% per year. This growth is fairly representative of CFD simulations applied throughout the industry. For comparison, Moore's Law has yielded about a 60% per year growth in computational power. The CFD community has matched this growth with a combination of growth in grid size for constant geometric complexity, growth in geometric complexity, growth in complexity of the flow physics being simulated, and growth in the number of cases and problems being supported by CFD simulations.

In closing, a remark is offered by the author. Workshops such as the DPW involve a lot of effort by a lot of dedicated people, much of it on their own time. With DPW, a balance is struck between rigorous testing and ease of participation. If requirements to participate are too strict, level of participation is diminished. If requirements are too relaxed, quality of data provided is degraded. Nonetheless, it would be beneficial to conduct a very rigorous numerical-prediction workshop that requires much tighter scrutiny of the data than that enforced by DPW, such as, ensuring that all residuals are converged to machine-level zero, that grid families are truly parametric, and that the building blocks of the methods have been verified by manufactured solutions, etc. Now, who is up for this task?

## References


1. 1st AIAA CFD Drag Prediction Workshop, Anaheim, CA, June 2001, http://aaac.larc.nasa.gov/tsab/cfdlarc/aiaa-dpw/Workshop1/workshop1.html.
2. Redeker, G., "DLR-F4 Wing-Body Configuration," *A Selection of Experimental Test Cases for the Validation of CFD Codes*, number AR-303, pages B4.1–B4.21. AGARD, August 1994.
3. Levy, D. W., Vassberg, J. C., Wahls, R. A., Zickuhr, T., Agrawal, S., Pirzadeh, S., and Hemsch, M. J., "Summary of data from the first AIAA CFD Drag Prediction Workshop," *AIAA Journal of Aircraft*, 40(5):875–882, Sep–Oct 2003.
4. Hemsch, M. J., "Statistical Analysis of CFD Solutions from the Drag Prediction Workshop," AIAA paper 2002-0842, 40th AIAA Aerospace Sciences Meeting & Exhibit, Reno, NV, January 2002.
5. Rakowitz, M., Eisfeld, B., Schwamborn, D., and Sutcliffe, M., "Structured and Unstructured Computations on the DLR-F4 Wing-Body Configuration," *AIAA Journal of Aircraft*, 40(2):256–264, 2003.
6. Mavriplis, D. J. and Levy, D. W., "Transonic Drag Predictions Using an Unstructured Multigrid Solver," *AIAA Journal of Aircraft*, 42(4):887–893, 2005.
7. Pirzadeh, S. Z. and Frink, N. T., "Assessment of the Unstructured Grid Software TetrUSS for Drag Prediction of the DLR-F4 Configuration," AIAA paper 2002-0839, 40th AIAA Aerospace Sciences Meeting & Exhibit, Reno, NV, January 2002.
8. Vassberg, J. C., Buning, P. G., and Rumsey, C. L., "Drag Prediction for the DLR-F4 Wing/Body Using OVERFLOW and CFL3D on an Overset Mesh," AIAA Paper 2002-0840, 40th AIAA Aerospace Sciences Meeting & Exhibit, Reno, NV, January 2002.
9. 2nd AIAA CFD Drag Prediction Workshop, Orlando, FL, June 2003, http://aaac.larc.nasa.gov/tsab/cfdlarc/aiaa-dpw/Workshop2/workshop2.html.
10. Laflin, K. R., Vassberg, J. C., Wahls, R. A., Morrison, J. H., Brodersen, O., Rakowitz, M., Tinoco, E. N., and Godard, J., "Summary of Data from the Second AIAA CFD Drag Prediction Workshop," *AIAA Journal of Aircraft*, 42(5):1165–1178, 2005.
11. Hemsch, M. and Morrison, J., "Statistical analysis of CFD solutions from 2nd Drag Prediction Workshop," AIAA Paper 2004-0556, 42nd AIAA Aerospace Sciences Meeting and Exhibit, Reno, NV, January 2004.
12. Pfeiffer, N., "Reflections on the Second Drag Prediction Workshop," AIAA Paper 2004-0557, 42nd AIAA Aerospace Sciences Meeting and Exhibit, Reno, NV, January 2004.
13. Brodersen, O. P., Rakowitz, M., Amant, S., Larrieu, P., Destarac, D., and Suttcliffe, M., "Airbus, ONERA and DLR Results from the Second AIAA Drag Prediction Workshop," *AIAA Journal of Aircraft*, 42(4):932–940, 2005.
14. Langtry, R. B., Kuntz, M., and Menter, F., "Drag Prediction of Engine-Airframe Interference Effects with CFX-5," *AIAA Journal of Aircraft*, 42(6):1523–1529, 2005.
15. Sclafani, J., DeHaan, M. A., and Vassberg, J. C., "OVERFLOW Drag Predictions for the DLR-F6 Transport Configuration: A DPW-II Case study," AIAA Paper 2004-0393, 42nd AIAA Aerospace Sciences Meeting and Exhibit, Reno, NV, January 2004.
16. Rumsey, C. Rivers, M., and Morrison, J., "Study of CFD Variations on Transport Configurations from the 2nd AIAA Drag Prediction Workshop," AIAA Paper 2004-0394, 42nd AIAA Aerospace Sciences Meeting and Exhibit, Reno, NV, January 2004.
17. Wutzler, K., "Aircraft Drag Prediction using Cobalt," AIAA Paper 2004-0395, 42nd AIAA Aerospace Sciences Meeting and Exhibit, Reno, NV, January 2004.
18. May, G., Van derWeide, E., Jameson, A., and Shankaran, S., "Drag Prediction of the DLR-F6 Configuration," AIAA Paper 2004-0396, 42nd AIAA Aerospace Sciences Meeting and Exhibit, Reno, NV, January 2004.
19. Kim, Y., Park, S., and Kwon, J., "Drag prediction of DLR-F6 using the turbulent Navier-Stokes calculations with multigrid," AIAA Paper 2004-0397, 42nd AIAA Aerospace Sciences Meeting and Exhibit, Reno, NV, January 2004.
20. Yamamoto, K., Ochi, A., Shima, E., and Takaki, R., "CFD Sensitivity to Drag prediction on DLR-F6 Configuration by Structured Method and Unstructured Method," AIAA Paper 2004-0398, 42nd AIAA Aerospace Sciences Meeting and Exhibit, Reno, NV, January 2004.
21. Tinoco, E. and Su, T., "Drag Prediction with the Zeus/CFL3D System," AIAA Paper 2004-0552, 42nd AIAA Aerospace Sciences Meeting and Exhibit, Reno, NV, January 2004.
22. 3rd AIAA CFD Drag Prediction Workshop, San Francisco, CA, June 2006, http://aaac.larc.nasa.gov/tsab/cfdlarc/aiaa-dpw/Workshop3/workshop3.html.
23. Vassberg, J. C., Sclafani, A. J., and DeHaan, M. A., "A Wing-Body Fairing Design for the DLR-F6 Model: A DPW-III Case Study," AIAA Paper 2005-4730, AIAA 23rd Applied Aerodynamics Conference, Toronto, Canada, June 2005.
24. Vassberg, J. C., Tinoco, E. N., Mani, M., Brodersen, O. P., Eisfeld, B., Wahls, R. A., Morrison, J. H., Zickuhr, T., Laflin, K. R., and Mavriplis, D. J., "Abridged Summary of the Third AIAA CFD Drag Prediction Workshop," *AIAA Journal of Aircraft*, 45(3):781–798, May–June 2008.
25. Vassberg, J. C., Tinoco, E. N., Mani, M., Brodersen, O. P., Eisfeld, B., Wahls, R. A., Morrison, J. H., Zickuhr, T., Laflin, K. R., and Mavriplis, D. J., "Summary of DLR-F6 Wing-Body Data from the Third AIAA CFD Drag Prediction Workshop," RTO AVT-147 Paper 57, RTO AVT-147 Symposium, Athens, Greece, December 2007.
26. Morrison, J. H. and Hemsch, M. J., "Statistical Analysis of CFD Solutions from the Third AIAA Drag Prediction Workshop," AIAA Paper 2007-0254, 45th AIAA Aerospace Sciences Meeting and Exhibit, Reno, NV, January 2007.

27. Tinoco, E. Winkler, N., C., Mani, M., and Venkatakrishnan, V., "Structured and Unstructured Solvers for the 3rd CFD Drag Prediction Workshop," AIAA Paper 2007-0255, 45th AIAA Aerospace Sciences Meeting and Exhibit, Reno, NV, January 2007.
28. Mavriplis, D. J., "Results from the 3rd Drag Prediction Workshop Using the NSU3D Unstructured Mesh Solver," AIAA Paper 2007-0256, 45th AIAA Aerospace Sciences Meeting and Exhibit, Reno, NV, January 2007.
29. Sclafani, A. J., Vassberg, J. C., Harrison, N. A., DeHaan, M. A., Rumsey, C. L., Rivers, S. M., and Morrison, J. H., "Drag Predictions for the DLR-F6 Wing/Body and DPW Wings Using CFL3D and OVERFLOW on an Overset Mesh," AIAA Paper 2007-0257, 45th AIAA Aerospace Sciences Meeting and Exhibit, Reno, NV, January 2007.
30. Brodersen, O., Eisfeld, B., Raddatz, J., and Frohnapfel, P., "DLR Results from the Third AIAA CFD Drag Prediction Workshop," AIAA Paper 2007-0259, 45th AIAA Aerospace Sciences Meeting and Exhibit, Reno, NV, January 2007.
31. Tinoco, E. N., Venkatakrishnan, V., Winkler, C., and Mani M., "Structured and Unstructured Solvers for the Third AIAA CFD Drag Prediction Workshop," *AIAA Journal of Aircraft*, 45(3):738–749, May–June 2008.
32. Mavriplis, D. J., "Third Drag Prediction Workshop Results Using NSU3D Unstructured Mesh Solver," *AIAA Journal of Aircraft*, 45(3):750–761, May–June 2008.
33. Sclafani, A. J., Vassberg, J. C., Harrison, N. A., Rumsey, C. L., Rivers, S. M., and Morrison, J. H., "CFL3D / OVERFLOW Results for DLR-F6 Wing/Body and Drag Prediction Workshop Wing," *AIAA Journal of Aircraft*, 45(3):762–780, May–June 2008.
34. Murayama, M. and Yamamoto, K., "Comparison Study of Drag Prediction by Structured and Unstructured Mesh Method," *AIAA Journal of Aircraft*, 45(3):799–822, May–June 2008.
35. Brodersen, O., Eisfeld, B., Raddatz, J., and Frohnapfel, P., "DLR results from the third AIAA Computational Fluid Dynamics Drag Prediction Workshop," *AIAA Journal of Aircraft*, 45(3):823–836, May–June 2008.
36. Eliasson, P. and Peng, S.-H., "Drag Prediction for the DLR-F6 Wing-Body Configuration Using the Edge Solver," *AIAA Journal of Aircraft*, 45(3):837–847, May–June 2008.
37. Mavriplis, D. J., Vassberg, J. C., Tinoco, E. N., Mani, M., Brodersen, O. P., Eisfeld, B., Wahls, R. H., Morrison, J., Zickuhr, T., Levy, D., and Murayama, M., "Grid quality and Resolution Issues from the Drag Prediction Workshop Series," *AIAA Journal of Aircraft*, 46(3):935–950, 2009.
38. 4th AIAA CFD Drag Prediction Workshop, San Antonio, TX, June 2009. http://aaac.larc.nasa.gov/tsab/cfdlarc/aiaa-dpw/Workshop4/workshop4.html, aiaadpw@gmail.com.
39. Vassberg, J. C., DeHaan, M. A., Rivers, S. M., and Wahls, R. A., "Development of a Common Research Model for Applied CFD Validation Studies," AIAA Paper 2008-6919, 26th AIAA Applied Aerodynamics Conference, Hawaii, HI, August 2008.
40. Rivers, M. and Dittberner, A., "Experimental Investigations of the NASA Common Research Model," AIAA Paper 2010-4218, 28th AIAA Applied Aerodynamics Conference, Chicago, IL, June 2010.
41. Rivers, M. and Dittberner, A., "Experimental Investigations of the NASA Common Research Model in the NASA Langley National Transonic Facility and NASA Ames 11-Ft Transonic Wind Tunnel (Invited)," AIAA Paper 2011-1126, presented at the 49th Aerospace Sciences Meeting, Orlando, FL, Jan 2011.
42. Common Research Model, http://commonresearchmodel.larc.nasa.gov/.
43. Vassberg, J., Tinoco, E., Mani, M., Rider, B., Zickuhr, T., Levy, D., Broderson, O., Eisfeld, B., Crippa, S., Wahls, R., Morrison, J., Mavriplis, D., Murayama, M., "Summary of the Fourth AIAA CFD Drag Prediction Workshop," AIAA 2010-4547, 28th AIAA Applied Aerodynamics Conference, Chicago, IL, June 2010.
44. Morrison, J., "Statistical Analysis of CFD Solutions from the Fourth Drag Prediction Workshop," AIAA 2010-4673, 28th AIAA Applied Aerodynamics Conference, Chicago, IL, June 2010.
45. Sclafani, A. J., Vassberg, J. C., Rumsey, C., DeHaan, M. A., and Pulliam, T. H., "Drag Prediction for the NASA CRM Wing/Body/Tail Using CFL3D and OVERFLOW on an Overset Mesh," AIAA Paper 2010-4219, 28th AIAA Applied Aerodynamics Conference, Chicago, IL, June 2010.
46. Hue, D., Gazaix, M., and Esquieu, S., "Computational Drag and Moment Prediction of the DPW4 Configuration with elsA," AIAA Paper 2010-4220, 28th AIAA Applied Aerodynamics Conference, Chicago, IL, June 2010.
47. Mani, M., Rider, B. J., Sclafani, A. J., Winkler, C., Vassberg, J. C., Dorgan, A. J., Cary, A., and Tinoco, E. N., "RANS Technology for Transonic Drag Prediction; a Boeing Perspective of the 4th Drag Prediction Workshop," AIAA Paper 2010-4221, 28th AIAA Applied Aerodynamics Conference, Chicago, IL, June 2010.
48. Yamamoto, K., Tanaka, K., and Murayama, M., "Comparison Study of Drag Prediction for the 4th CFD Drag Prediction Workshop Using Structured and Unstructured Mesh Methods," AIAA Paper 2010-4222, 28th AIAA Applied Aerodynamics Conference, Chicago, IL, June 2010.
49. Brodersen, O., Crippa, S., Eisfeld, B., Keye, S., and Geisbauer, S., "DLR Results for the Fourth AIAA CFD Drag Prediction Workshop," AIAA Paper 2010-4223, 28th AIAA Applied Aerodynamics Conference, Chicago, IL, June 2010.
50. Eliasson, P., Peng, S., and Tysell, L., "Computations from the 4th Drag Prediction Workshop Using the Edge solver," AIAA Paper 2010-4548, 28th AIAA Applied Aerodynamics Conference, Chicago, IL, June 2010.
51. Li, G. and Zhou, Z., "Validation of a Multigrid-Based Navier-Stokes Solver for Transonic Flows," AIAA Paper 2010-4549, 28th AIAA Applied Aerodynamics Conference, Chicago, IL, June 2010.
52. Mavriplis, D. J. and Long, M., "NSU3D Results for the Fourth AIAA Drag Prediction Workshop," AIAA Paper 2010-4550, 28th AIAA Applied Aerodynamics Conference, Chicago, IL, June 2010.

53. Lee-Rausch, E., Hammond, E., Nielsen, E., Pirzadeh, S., and Rumsey C., "Application of the FUN3D Unstructured-Grid Navier-Stokes Solver to the 4th AIAA Drag Prediction Workshop Cases," AIAA Paper 2010-4551, 28th AIAA Applied Aerodynamics Conference, Chicago, IL, June 2010.
54. Vos, J., Sanchi, S., Gehri, A., and Stephani, P., "DPW4 Results Using Different Grids, Including Near-Field/Far-Field Drag Analysis," AIAA Paper 2010-4552, 28th AIAA Applied Aerodynamics Conference, Chicago, IL, June 2010.
55. Hashimoto, A., Lahur, P., Murakami, K., and Aoyama, T., "Validation of Fully Automatic Grid Generation Method on Aircraft Drag Prediction," AIAA Paper 2010-4669, 28th AIAA Applied Aerodynamics Conference, Chicago, IL, June 2010.
56. Temmerman, L. and Hirsch, C., "Simulations of the CRM Configuration on Unstructured Hexahedral Grids: Lessons Learned from the DPW-4 Workshop," AIAA Paper 2010-4670, 28th AIAA Applied Aerodynamics Conference, Chicago, IL, June 2010.
57. Chaffin, M. and Levy, D., "Comparison of Viscous Grid Layer Growth Rate of Unstructured Grids on CFD Drag Prediction Workshop Results," AIAA Paper 2010-4671, 28th AIAA Applied Aerodynamics Conference, Chicago, IL, June 2010.
58. Crippa, S., "Application of Novel Hybrid Mesh Generation Methodologies for Improved Unstructured CFD Simulations," AIAA Paper 2010-4672, 28th AIAA Applied Aerodynamics Conference, Chicago, IL, June 2010.
59. 5th AIAA CFD Drag Prediction Workshop, http://aaac.larc.nasa.gov/tsab/cfdlarc/aiaa-dpw/, aiaadpw@gmail.com.
60. Vassberg, J. C., "A Unified Baseline Grid about the Common Research Model Wing-Body for the Fifth AIAA CFD Drag Prediction Workshop," AIAA Paper 2011-3508, 29th AIAA Applied Aerodynamics Conference, Honolulu, HI, June 2011.
61. Rumsey, C., "Langley Research Center Turbulence Modeling Resource", http://turbmodels.larc.nasa.gov/.
62. Rivers, M. and Hunter, C., "Support System Effects on the NASA Common Research Model," AIAA Paper 2012-0707, January 2012.
63. Rivers, M., Hunter, C., and Campbell, R., "Further Investigation of the Support System Effects and Wing Twist on the NASA Common Research Model," AIAA Paper 2012-3209, June 2012.
64. Levy, D. W., Laflin, K. R., Tinoco, E. N., Vassberg, J. C., Mani, M., Rider, B., Rumsey, C. L., Wahls, R. A., Morrison, J. H., Brodersen, O. P., Crippa, S., Mavriplis, D. J., and Murayama, M., "Summary of Data from the Fifth AIAA CFD Drag Prediction Workshop," AIAA Paper 2013-0046, AIAA 51st Aerospace Sciences Meeting, Grapevine, TX, January, 2013.
65. Morrison, J. H., "Statistical Analysis of CFD solutions from the Fifth AIAA Drag Prediction Workshop," AIAA Paper 2013-0047, AIAA 51st Aerospace Sciences Meeting, Grapevine, TX, January, 2013.
66. Sclafani, A. J., Vassberg, J. C., Winkler, C., Dorgan, A. J., Mani, M., Olsen, M. E., and Coder, J. G., "DPW-5 Analysis of the CRM in a Wing-Body Configuration Using Structured and Unstructured Meshes," AIAA Paper 2013-0048, AIAA 51st Aerospace Sciences Meeting, Grapevine, TX, January, 2013.
67. Murayama, M., Yamamoto, K., Hashimoto, A., Ishida, T., Uenoand, M., Tanaka, K., and Ito, Y., "Summary of JAXA Studies for the Fifth AIAA CFD Drag Prediction Workshop using UPACS and FaSTAR," AIAA Paper 2013-0049, AIAA 51st Aerospace Sciences Meeting, Grapevine, TX, January, 2013.
68. Park, M. A., Laflin, K. R., Chaffin, M. S., Powell, N., and Levy, D. W., "CFL3D, FUN3D, and NSU3D Contributions to the Fifth Drag Prediction Workshop," AIAA Paper 2013-0050, AIAA 51st Aerospace Sciences Meeting, Grapevine, TX, January, 2013.
69. Ceze, M., and Fidkowski, K. J., "Drag Prediction using Adaptive Discontinuous Finite Elements," AIAA Paper 2013-0051, AIAA 51st Aerospace Sciences Meeting, Grapevine, TX, January, 2013.
70. Scalabrin, L. C., and de Souza, R. F., "Grid Assessment using the NASA Common Research Model (CRM) Wind Tunnel Data," AIAA Paper 2013-0052, AIAA 51st Aerospace Sciences Meeting, Grapevine, TX, January, 2013.
71. Gariepy, M., Malouin, B., Trepanier, J.-Y., and Laurendeau, E., "Far-Field Drag Decomposition Method Applied to the DPW-5 Test Case Results," AIAA Paper 2013-2507.
72. Vassberg, J. C., and Lee-Rausch, B., Guest Editors, "Special Section: Drag Prediction Workshop, A selection of 21 papers from DPW-IV and DPW-V," *AIAA Journal of Aircraft*, 51(4):1069-1343, July-August 2014.

**Table 1. Reference quantities for the CRM.**

| | | | | | |
|---|---|---|---|---|---|
| $S_{ref}$ | 594,720.0 $in^2$ | = 4,130 $ft^2$ [458.89 $m^2$] | $x_{ref}$ | 1,325.9 in | [33.68 m] |
| $S_{trap}$ | 576,000.0 $in^2$ | = 4,000 $ft^2$ [444.44 $m^2$] | $y_{ref}$ | 468.75 in | [11.91 m] |
| b | 2,313.5 in | = 192.8 ft [58.765 m] | $z_{ref}$ | 177.95 in | [4.520 m] |
| $C_{ref}$ | 275.800 in | = 16.07 ft [4.8978 m] | $\Lambda_{c/4}$ | 35.0° | |
| AR | 9.0 | | $\lambda$ | 0.275 | |

**Table 2. Gridding guidelines (from DPW-IV).**

1) Initial spacing normal to all viscous walls (RE Based on $C_{ref}$= 275.80"):
   a) coarse: $y^+ \sim 1.0$ $\Delta y_1$= 0.001478 (RE= 5M)
   b) medium: $y^+ \sim 2/3$ $\Delta y_1$= 0.000985 (RE= 5M), $\Delta y_1$= 0.000273 (RE= 20M)
   c) fine: $y^+ \sim 4/9$ $\Delta y_1$= 0.000657 (RE= 5M)
   d) extra-fine: $y^+ \sim 8/27$ $\Delta y_1$= 0.000438 (RE= 5M)
2) Recommended: generate grids with 2 cell layers of constant spacing normal to viscous walls
3) Total grid size to grow ~3X between each grid level for grid convergence cases
4) For structured meshes, this growth is ~1.5X in each coordinate direction
5) Grid convergence cases must maintain the same grid family between grid levels, i.e. maintain the same stretching factors, same topology, etc.
6) Growth rate of cell sizes in the viscous layer should be < 1.25.
7) Far field located at ~100 $C_{refs}$ for all grid levels.
8) For the Medium Baseline Grids:
   a) Chordwise spacing for wing and tail leading edge (LE) and trailing edge (TE) ~0.1% local chord.
   b) Wing and tail Spanwise spacing at root ~0.1% local semispan.
   c) Wing and tail Spanwise spacing at tip ~0.1% local semispan.
   d) Cell size near fuselage nose and after-body ~2.0% $C_{ref}$.
9) For the Coarse and Fine Baseline Grids, the above values should be scaled accordingly.
10) Wing and Tail Trailing Edge Base:
   a) Minimum of 8 cells across TE base for the coarse mesh
   b) Minimum of 12 cells across TE base for the medium mesh
   c) Minimum of 16 cells across TE base for the fine mesh
   d) Minimum of 24 cells across TE base for the extra-fine mesh
11) Be multi-grid friendly
12) For unstructured grids designed for vertex based solvers, the spacings refer to inter-nodal spacings and the resulting grid sizes are expected to be similar to the structured grid sizes above. For unstructured grids for cell-centered solvers, the spacings refer to spacings between cell centers (or surface face centers), which corresponds approximately to a factor of 2 reduction in the overall number of surface points compared to the nodal solver case, for a triangular surface grid (this is based on triangle centroid separation distance of 2/3h). For tetrahedral cell-centered-solver meshes, the total number of grid points will be approximately 1/3 of the numbers listed above.

**Table 3. Metric parameters for the common grids (counts in millions).**

| | | | | Multiblock Structured | | Overset | Unstr. Hex | | Unstr. Prism | | Unstr. Hybrid | | |
|---|---|---|---|---|---|---|---|---|---|---|---|---|---|
| **Level** | **Name** | **Label** | $\Delta_1 y^+$ | **Cells** | **Nodes** | **Points** | **Cells** | **Nodes** | **Cells** | **Nodes** | **Tets** | **Prism** | **Nodes** |
| 1 | Tiny | T | 2.00 | 0.64 | 0.66 | 0.8 | 0.64 | 0.66 | 1.3 | 0.66 | 2.6 | 0.43 | 0.66 |
| 2 | Coarse | C | 1.33 | 2.2 | 2.2 | 2.5 | 2.2 | 2.2 | 4.3 | 2.2 | 8.6 | 1.4 | 2.2 |
| **3** | **Medium** | **M** | **1.00** | **5.1** | **5.2** | **5.7** | **5.1** | **5.2** | **10.2** | **5.2** | **20.8** | **3.3** | **5.2** |
| 4 | Fine | F | 0.67 | 17.3 | 17.4 | 18.6 | 17.3 | 17.4 | 34.5 | 17.4 | 69.7 | 11.3 | 17.4 |
| 5 | Extra Fine | X | 0.50 | 40.9 | 41.2 | 43.3 | 40.9 | 41.2 | 81.8 | 41.2 | 166.1 | 26.4 | 41.2 |
| 6 | Super Fine | S | 0.33 | 138.0 | 138.8 | 143.5 | 138.0 | 138.8 | --- | --- | --- | --- | --- |

**Table 4. DPW-V case 1 and 2 submissions and participant data key.**

| Team | ID | Name | Organization | Code | Misc Solver | Grid Type | Turbulence Model |
|---|---|---|---|---|---|---|---|
| 1 | A | Sclafani | Boeing (Huntington) | OVERFLOW v2.2c | Central | Overset | SA-Ia |
| | B | Sclafani | Boeing (Huntington) | OVERFLOW v2.2c | Central | Overset | SA-Ia w/ RC |
| | C | Sclafani | Boeing (Huntington) | OVERFLOW v2.2c | Central | Custom (Overset) | SA-Ia |
| | D | Sclafani | Boeing (Huntington) | OVERFLOW v2.2c | Central / QCR | Custom (Overset) | SA-Ia |
| | E | Sclafani | Boeing (Huntington) | OVERFLOW v2.2c | Central | Custom (Overset) | SA-Ia w/ RC |
| | F | Sclafani | Boeing (Huntington) | OVERFLOW v2.2c | Central / QCR | Custom (Overset) | SA-Ia w/ RC |
| | G | Sclafani | Boeing (Huntington) | OVERFLOW v2.2c | Central | Custom (Overset) | SA-Ia w/ RC |
| | H | Sclafani | Boeing (Huntington) | OVERFLOW v2.2c | Central / QCR | Custom (Overset) | SA-Ia w/ RC |
| 2 | I | Chen | CADRC | MFlow | Upwind | Hex | SA |
| | J | Chen | CARDC | MFlow | Upwind | Hybrid | SA |
| 3 | K | GariÈpy | EcolePolytechMontreal | Fluent V13 | Upwind | Prism | SA |
| | L | GariÈpy | EcolePolytechMontreal | Fluent V13 | Upwind | Custom (Hex) | SA |
| 4 | M | Scalabrin | Embraer | CFD++ | Upwind | Hex | RT |
| | N | Scalabrin | Embraer | CFD++ | Upwind | Hex | SST |
| | O | Scalabrin | Embraer | CFD++ | Upwind | Hybrid | RT |
| | P | Scalabrin | Embraer | CFD++ | Upwind | Hybrid | SST |
| | Q | Scalabrin | Embraer | CFD++ | Upwind | Prism | RT |
| | R | Scalabrin | Embraer | CFD++ | Upwind | Prism | SST |
| | S | Scalabrin | Embraer | CFD++ | Upwind | Custom (Hybrid) | RT |
| | T | Scalabrin | Embraer | CFD++ | Upwind | Custom (Hybrid) | SST |
| 5 | U | Eliasson | FOI | EDGE | Central | Hex | EARSM |
| | V | Eliasson | FOI | EDGE | Central | Hex | SA |
| | W | Eliasson | FOI | EDGE | Central | Hex | SST |
| 6 | X | Powell | Gulfstream * | FUN3D | Upwind Roe | Hybrid | SA |
| 7 | Y | Balakrishnan | Indian Inst. Science | HiFUN | Upwind | Hex | SA |
| 8 | Z | Hashimoto | JAXA * | FaSTAR | Upwind | Hex | SA-noft2-R |
| | 2 | Hashimoto | JAXA | FaSTAR | Upwind | Custom (Hex) | SA-noft2-R |
| 9 | 3 | Yamamoto | JAXA * | UPACS | Upwind | Multi-block | SA-noft2-R (Crot=1) |
| | 4 | Yamamoto | JAXA * | UPACS | Upwind | Multi-block | SST-V |
| 10 | 5 | Olson | NASA Ames * | overflow2.2e_LRS | Central/matrix | Overset | Lag RST |
| 11 | 6 | Park | NASA Langley | FUN3D v12.2 | Upwind Roe | Hybrid | SA |
| | 7 | Park | NASA Langley | CFL3D v6.6 | Upwind Roe | Multi-block | SA |
| 12 | 8 | Cai | NPU China * | ExStream | Upwind | Overset | SST |
| 13 | 9 | Hue | ONERA | elsA | Central | Multi-block | SA |
| 14 | a | Coder | Penn St. U | OVERFLOW 2.2c | Upwind | Overset | SA-fv3 |
| 15 | b | Osusky | U. Toronto * | Diablo | Scalar | Multi-block | SA |
| | d | Osusky | U. Toronto * | Diablo | Matrix | Multi-block | SA |
| 16 | e | Levy | Cessna Aircraft Co. * | NSU3D | Central/matrix | Hybrid | SA |
| | f | Levy | Cessna Aircraft Co. | FUN3D | Upwind Roe | Hybrid | SA |
| 17 | g | Crippa | DLR | TAU | Matrix | Hex | SA |
| | h | Crippa | DLR | TAU | Matrix | Hex | SST |
| 18 | k | Moitra | CRL_INDIA | CFD++ | Upwind | Prism | SA-RC |
| 19 | m | Winkler | Boeing (St. Louis) | BCFD | Upwind HLLE | Hex | SA |
| | n | Winkler | Boeing (St. Louis) | BCFD | Upwind HLLE | Hex | SST-V |
| | q | Winkler | Boeing (St. Louis) | BCFD | Upwind HLLE | Hex | SA |
| | r | Winkler | Boeing (St. Louis) | BCFD | Upwind HLLE | Hex | SST-V |
| 20 | t | Temmerman | NUMECA | FINE/Open | Cell Centered | Multi-block | SA |
| 21 | α | Brodersen | DLR | TAU | Diss 1 | Custom (Hybrid) | SA |
| | β | Brodersen | DLR | TAU | Diss 3 | Custom (Hybrid) | SA |
| | δ | Brodersen | DLR | TAU | Diss 1 | Custom (Hyb w/Hex-Wake) | SA |
| | γ | Brodersen | DLR | TAU | Diss 3 | Custom (Hyb w/Hex-Wake) | SA |
| | λ | Brodersen | DLR | TAU | Diss 1 | Custom (Hyb w/Hex-Wake) | Menter SST |
| | π | Brodersen | DLR | TAU | Diss 3 | Custom (Hyb w/Hex-Wake) | Menter SST |
| 6 | ξ | Powell | Gulfstream ** | FUN3D | Upwind Roe | Custom (Tet) | SA |
| | ψ | Powell | Gulfstream ** | USM3D | Upwind Roe | Custom (Tet) | SA |
| 9 | σ | Yamamoto | JAXA ** | UPACS | Upwind Roe | Custom (MB) | SA-noft2-R (Crot=1) |
| | ϖ | Yamamoto | JAXA ** | UPACS | Upwind Roe | Custom (MB) | SST-V |

* Data Resubmitted After Workshop ** Cases Added After Workshop

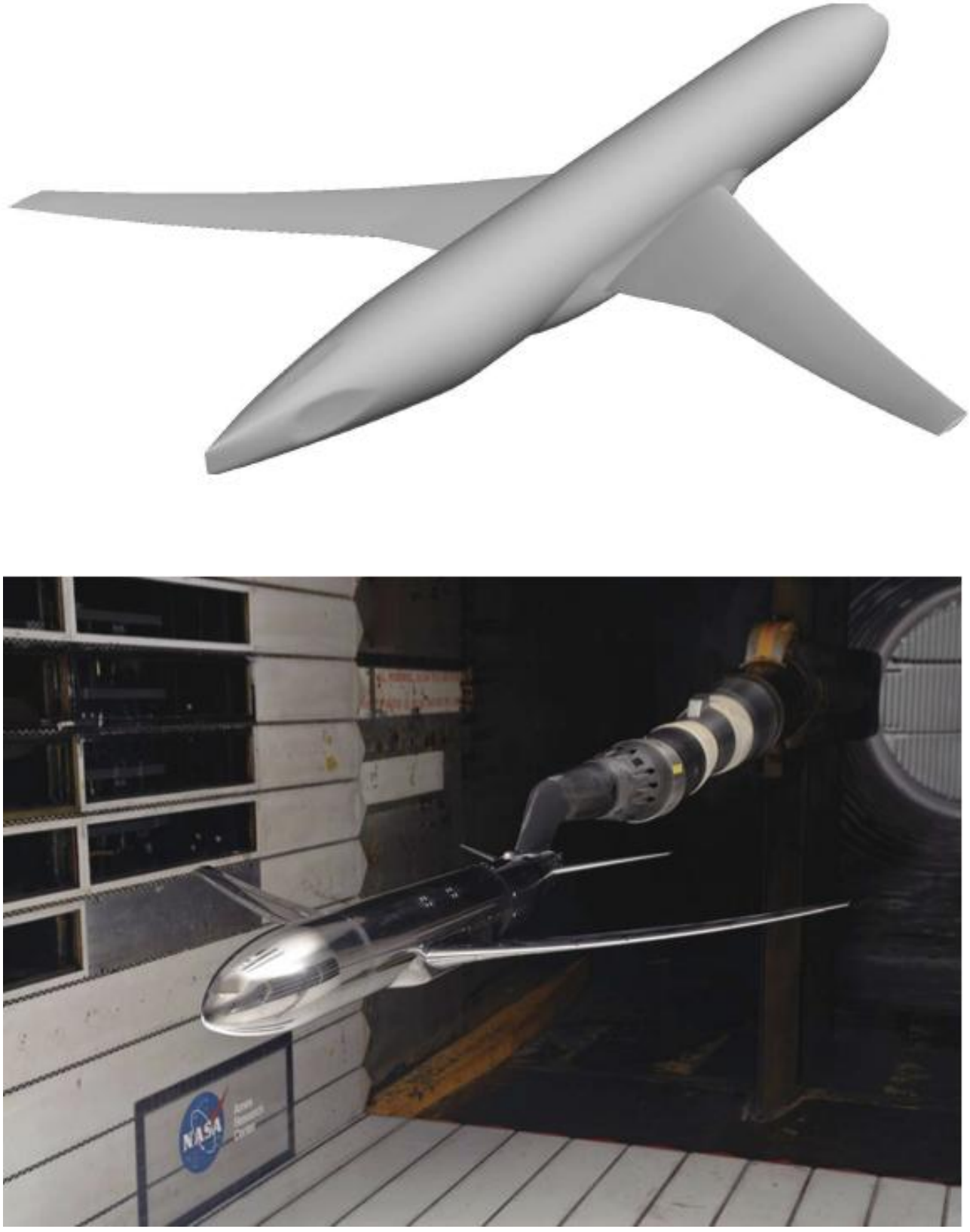


**Figure 1. NASA Common Research Model (CRM) geometry for DPW-V.**

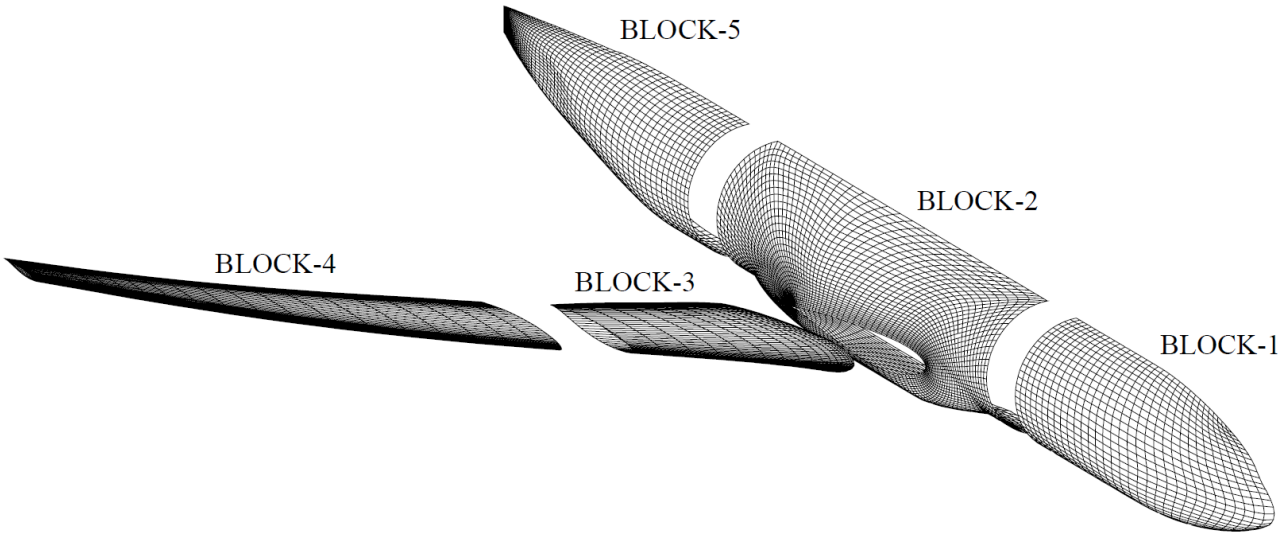


**Figure 2. Block topology for the CRM wing/body multiblock grid family.**

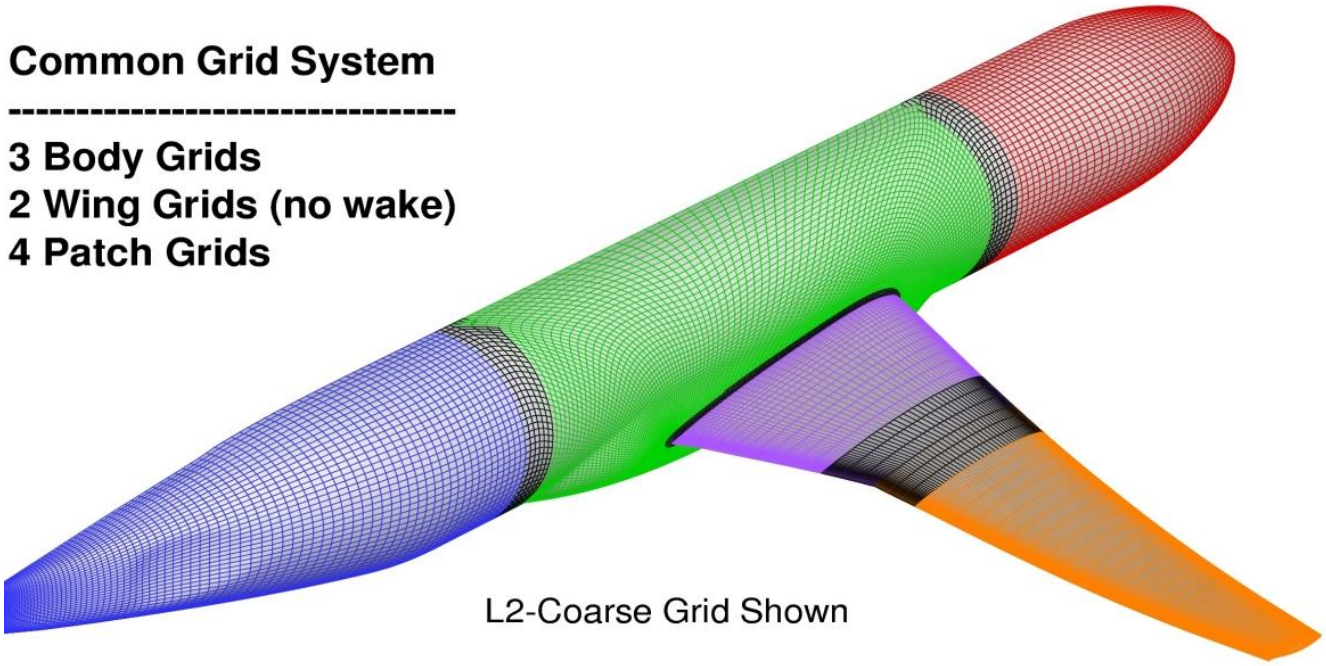


**Figure 3. Overset patch grids derived from the multiblock structured grid.**

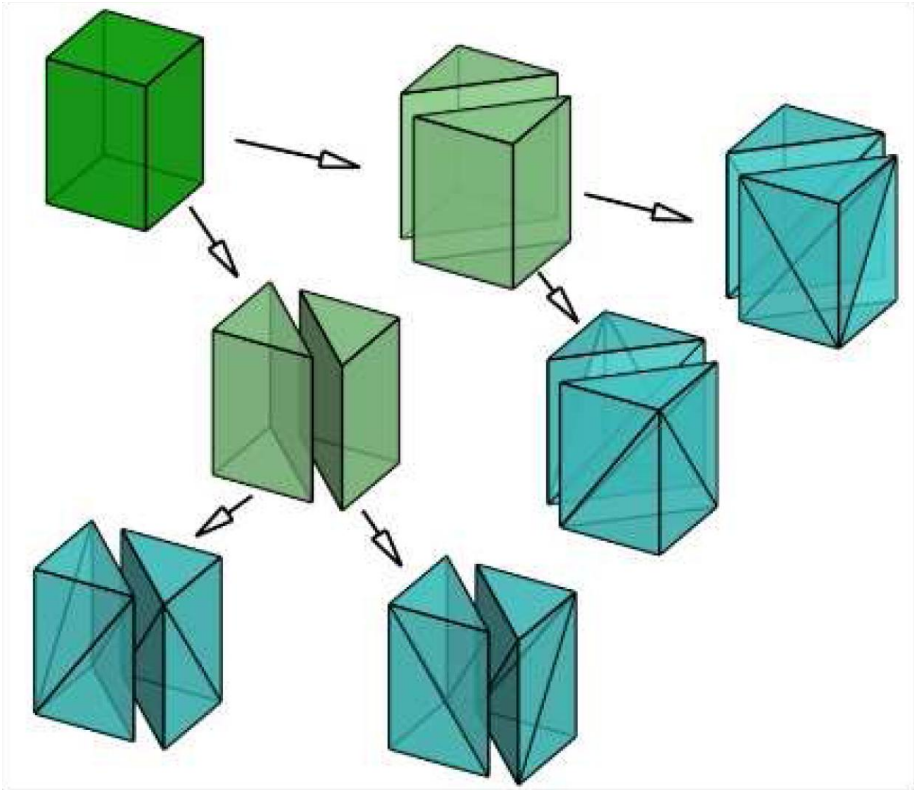

a) Hex to prisms and tetrahedral

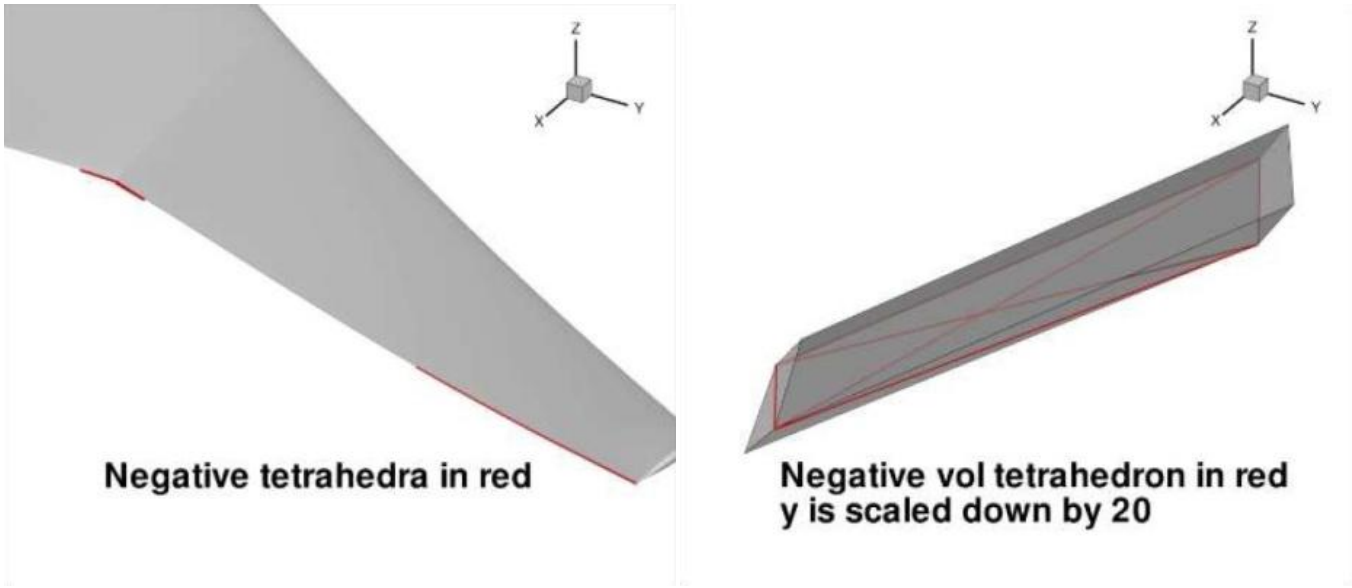


b) Issues with distorted high aspect ratio cells

**Figure 4. Unstructured grids derived from the multiblock structured grid.**

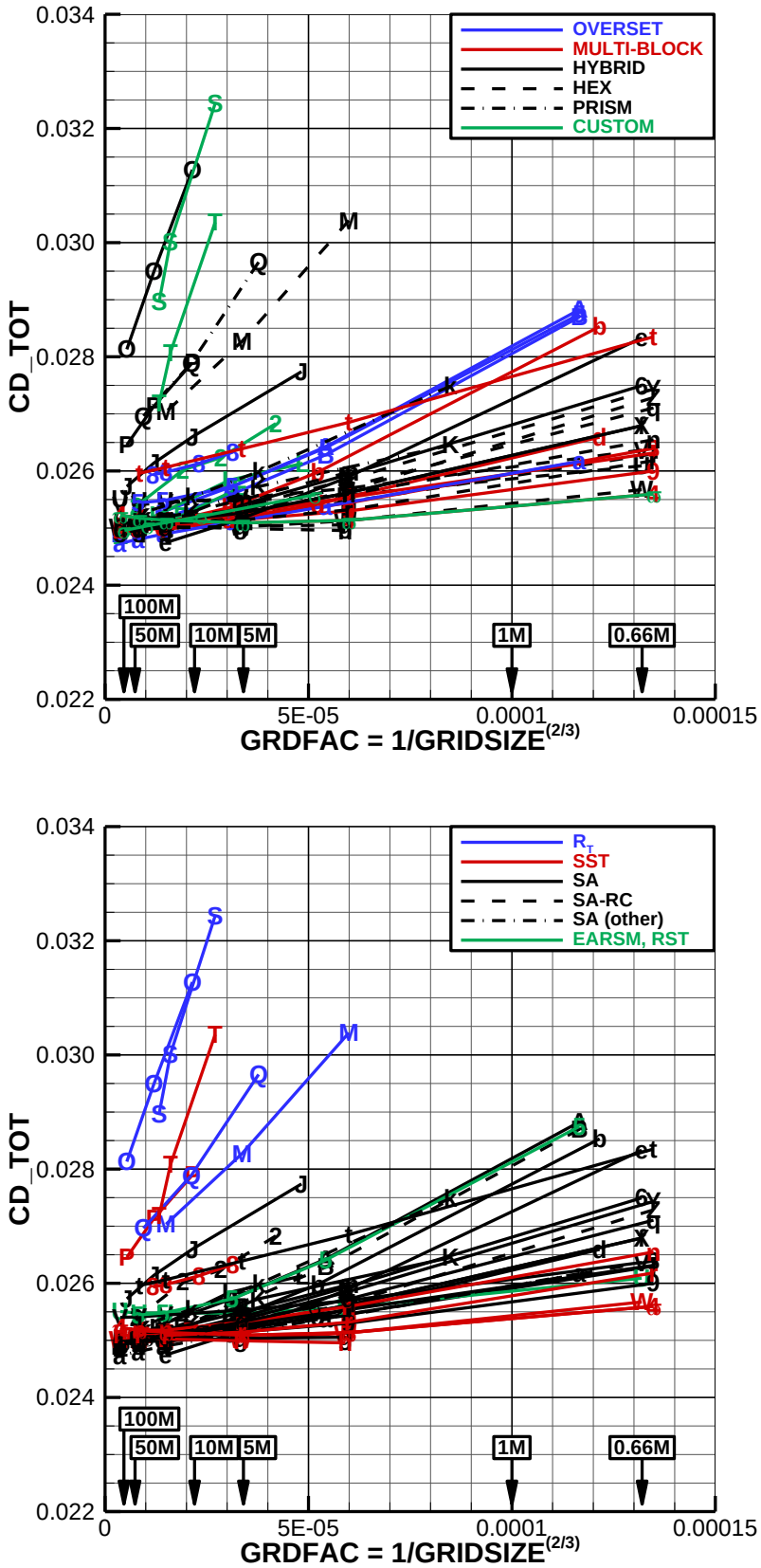


**Figure 5. Case 1 total drag by grid type and turbulence model.**

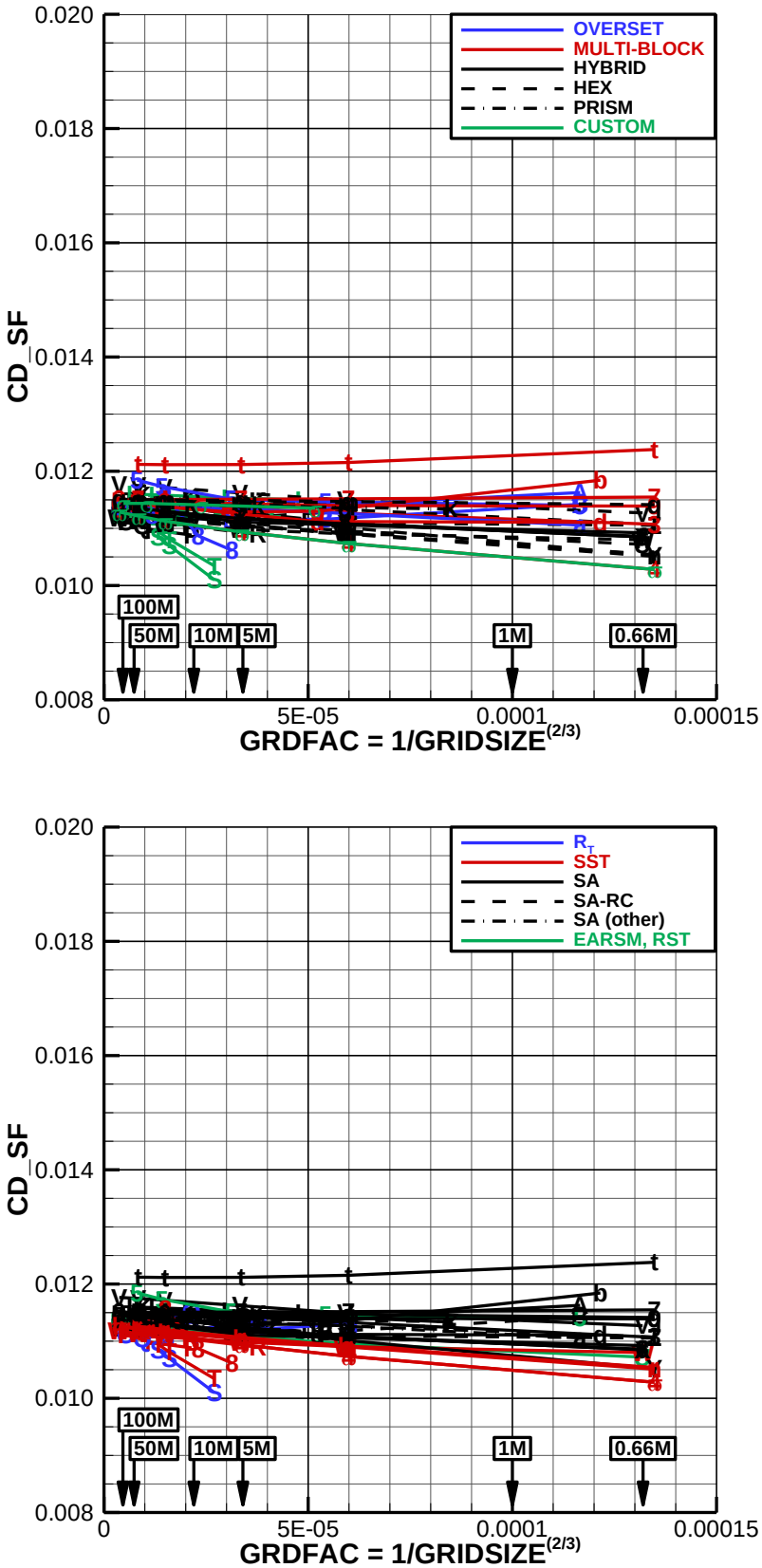


**Figure 6. Case 1 skin friction drag by grid type and turbulence model.**

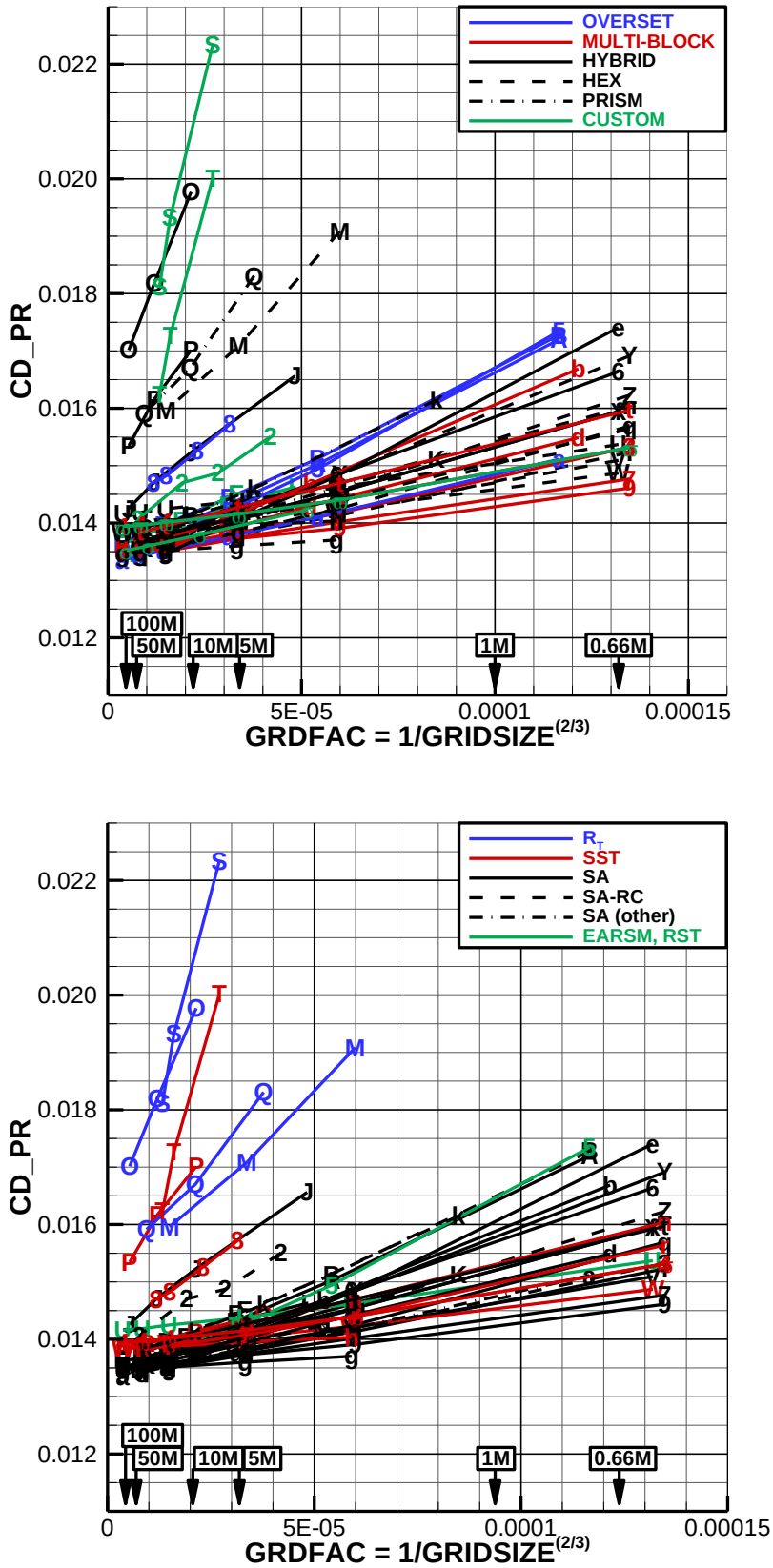


**Figure 7. Case 1 pressure drag by grid type and turbulence model.**

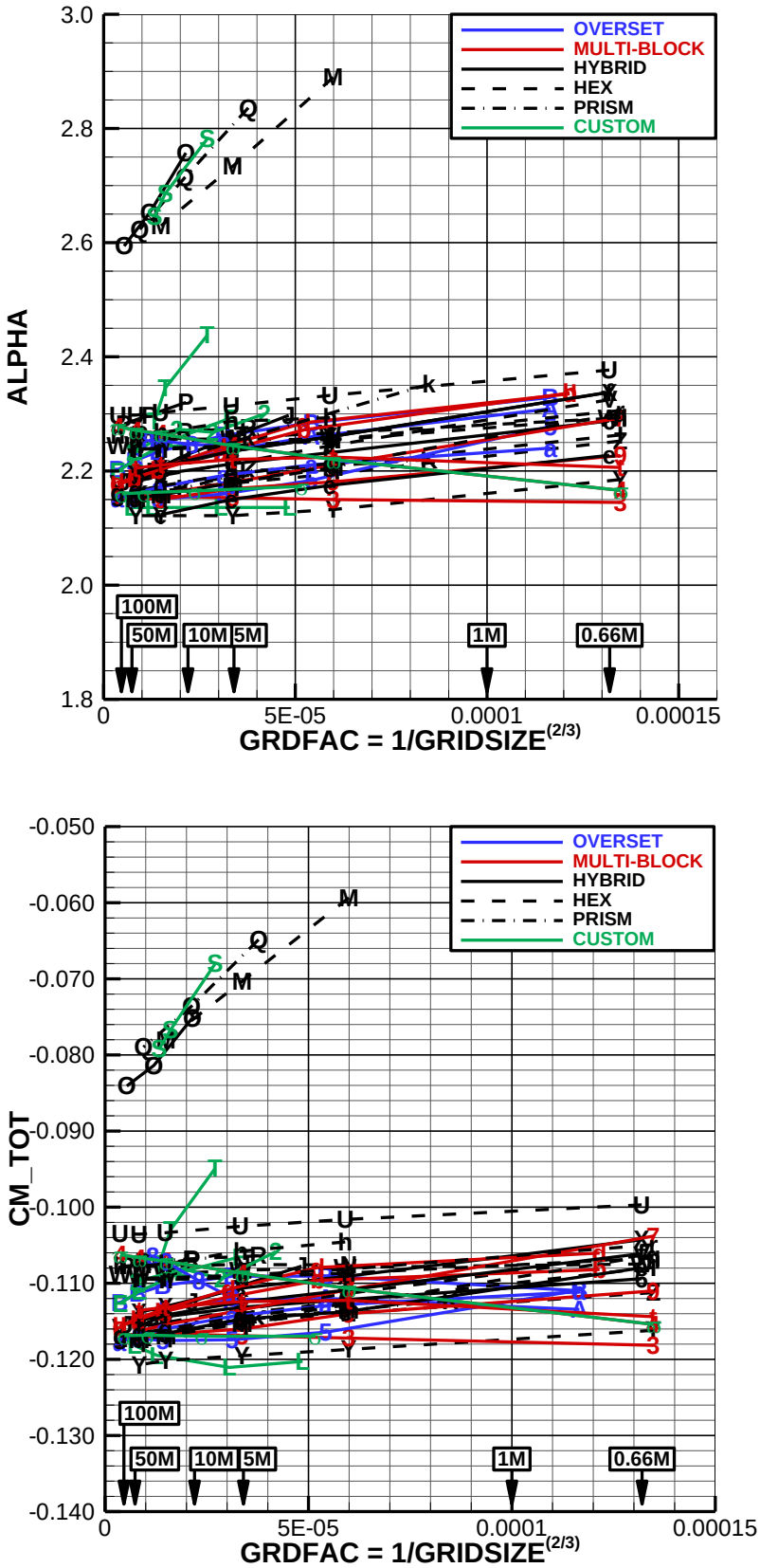


**Figure 8. Case 1 alpha and pitching moment by grid type.**

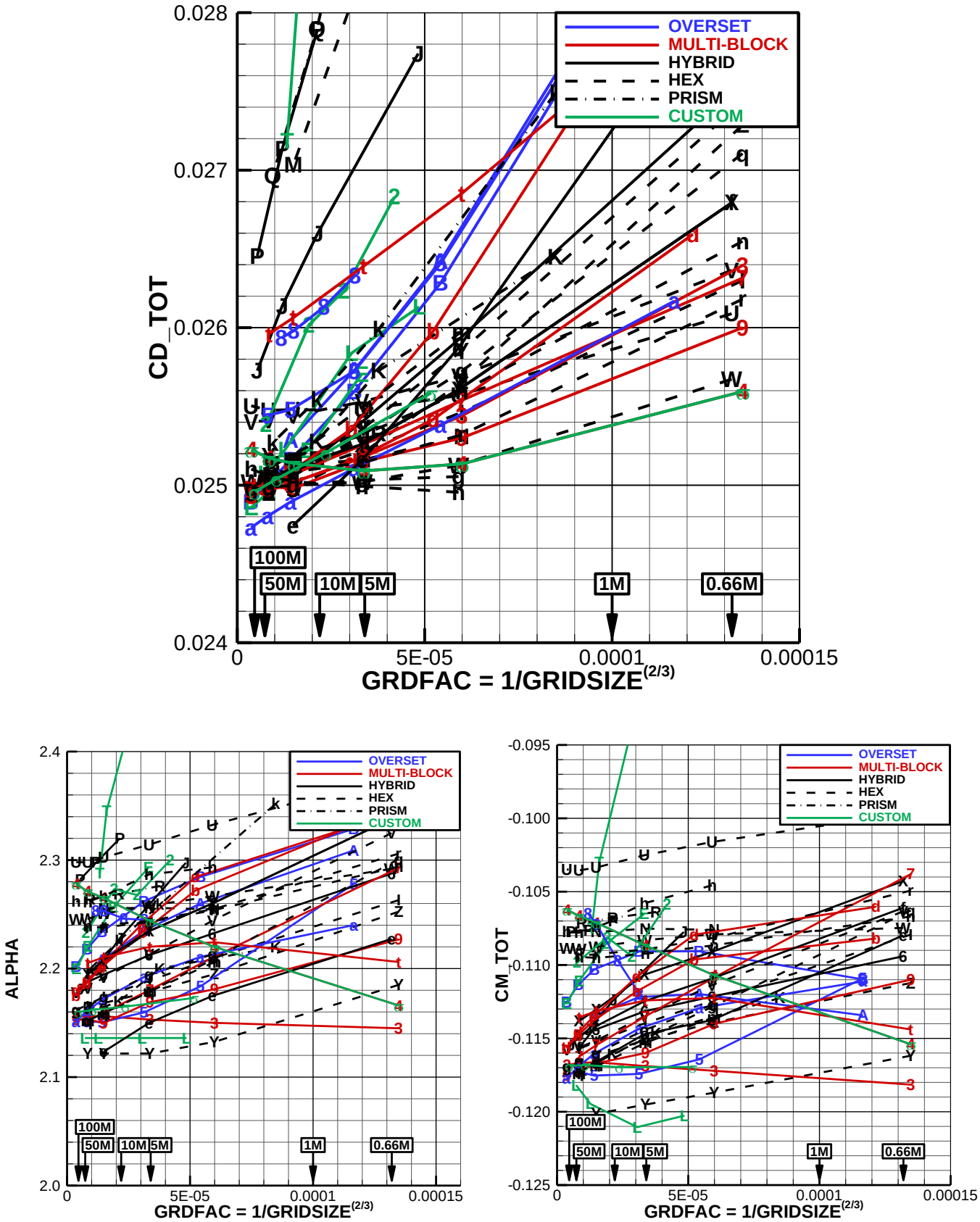


**Figure 9. Case 1 total drag, alpha, and pitching moment by grid type: expanded scale.**

Wind Tunnel Results shown for Reference Only

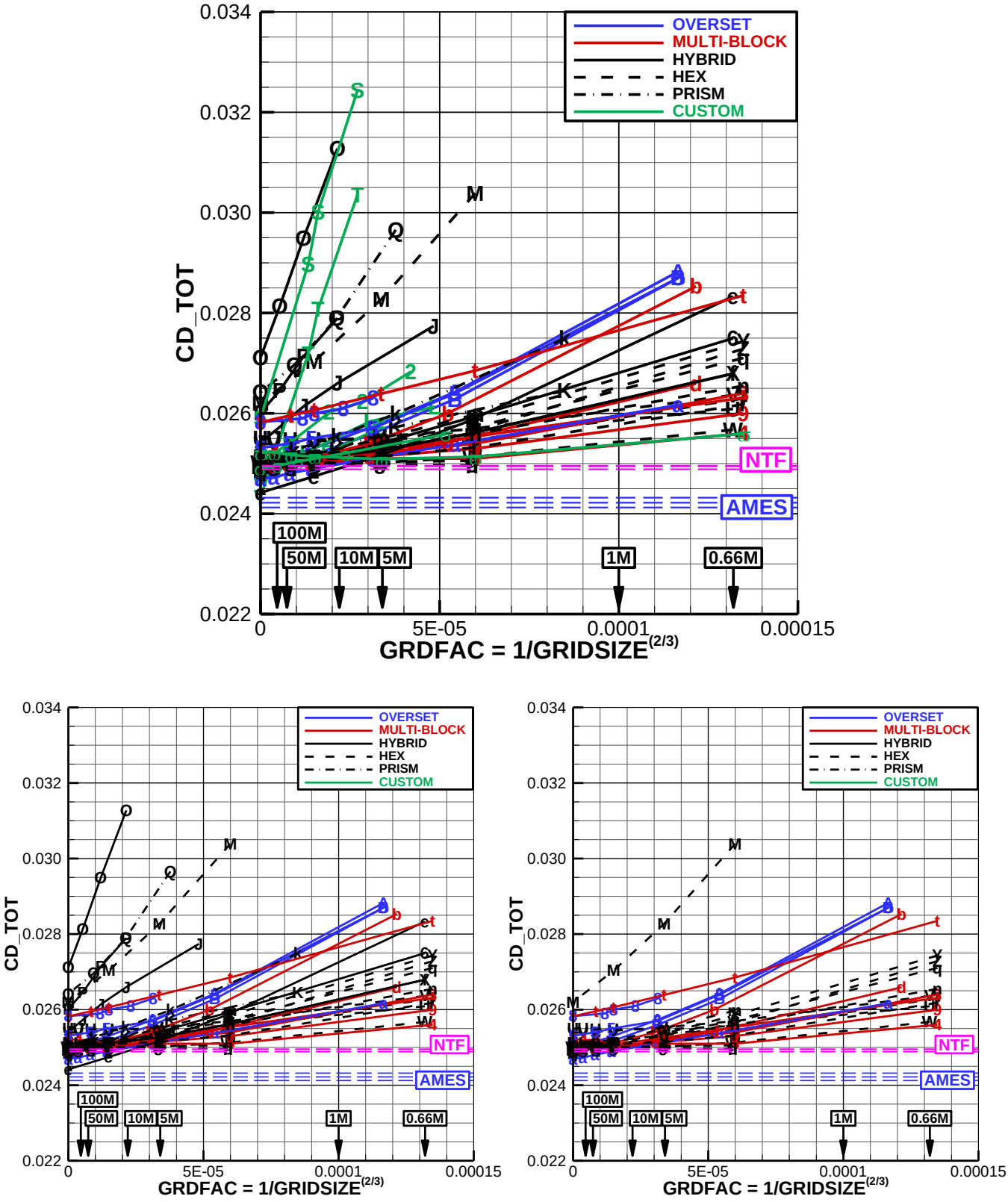


**Figure 10. Case 1 total drag Richardson extrapolation with wind tunnel data.**

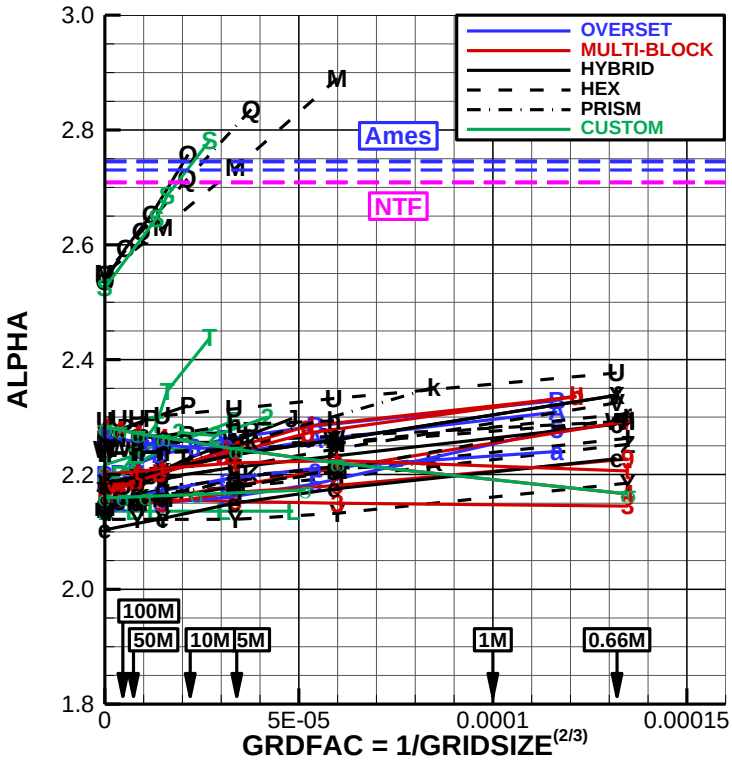


a) ALPHA: All Grids

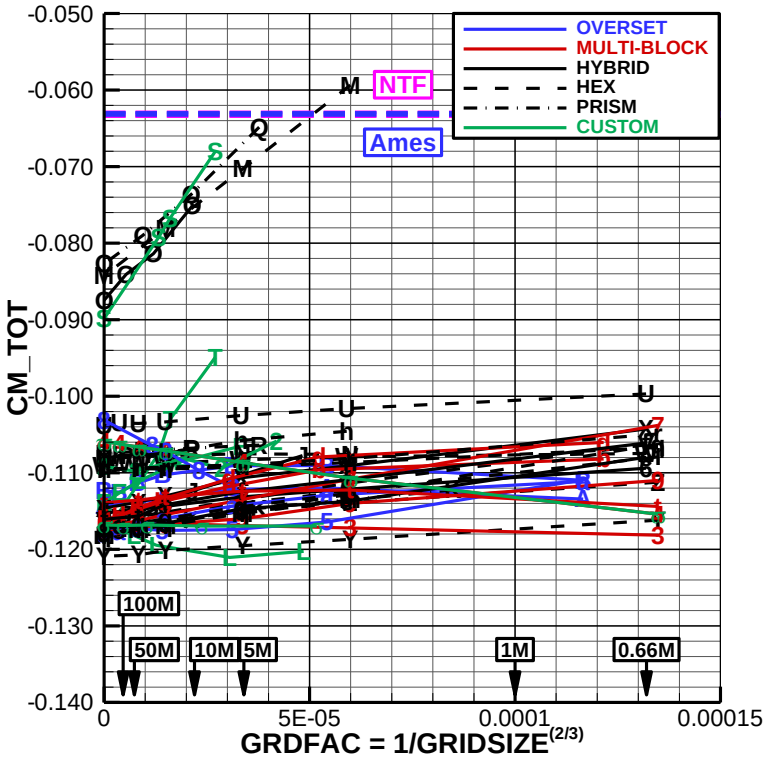


b) CM_TOT: All Grids

**Figure 11. Case 1 alpha and pitching moment Richardson extrapolation with wind tunnel data.**

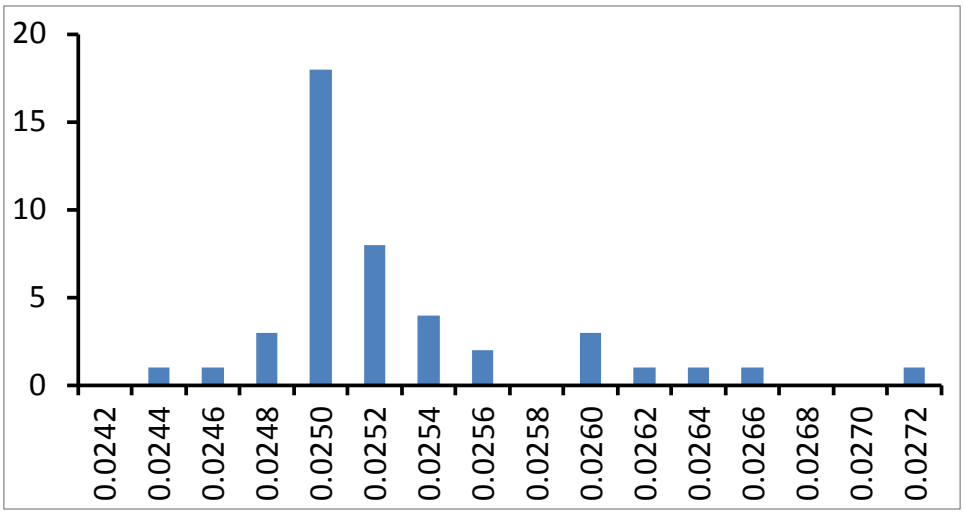


**Distribution of continuum total drag**

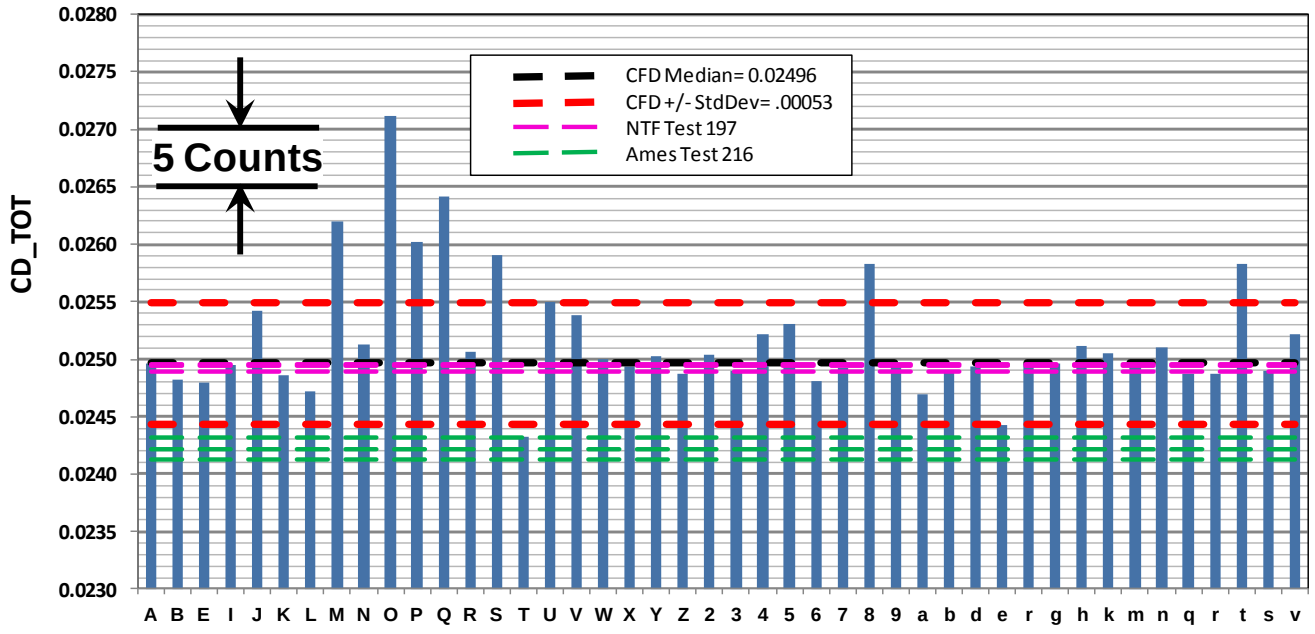


**Figure 12. Case 1 total drag continuum extrapolation.**

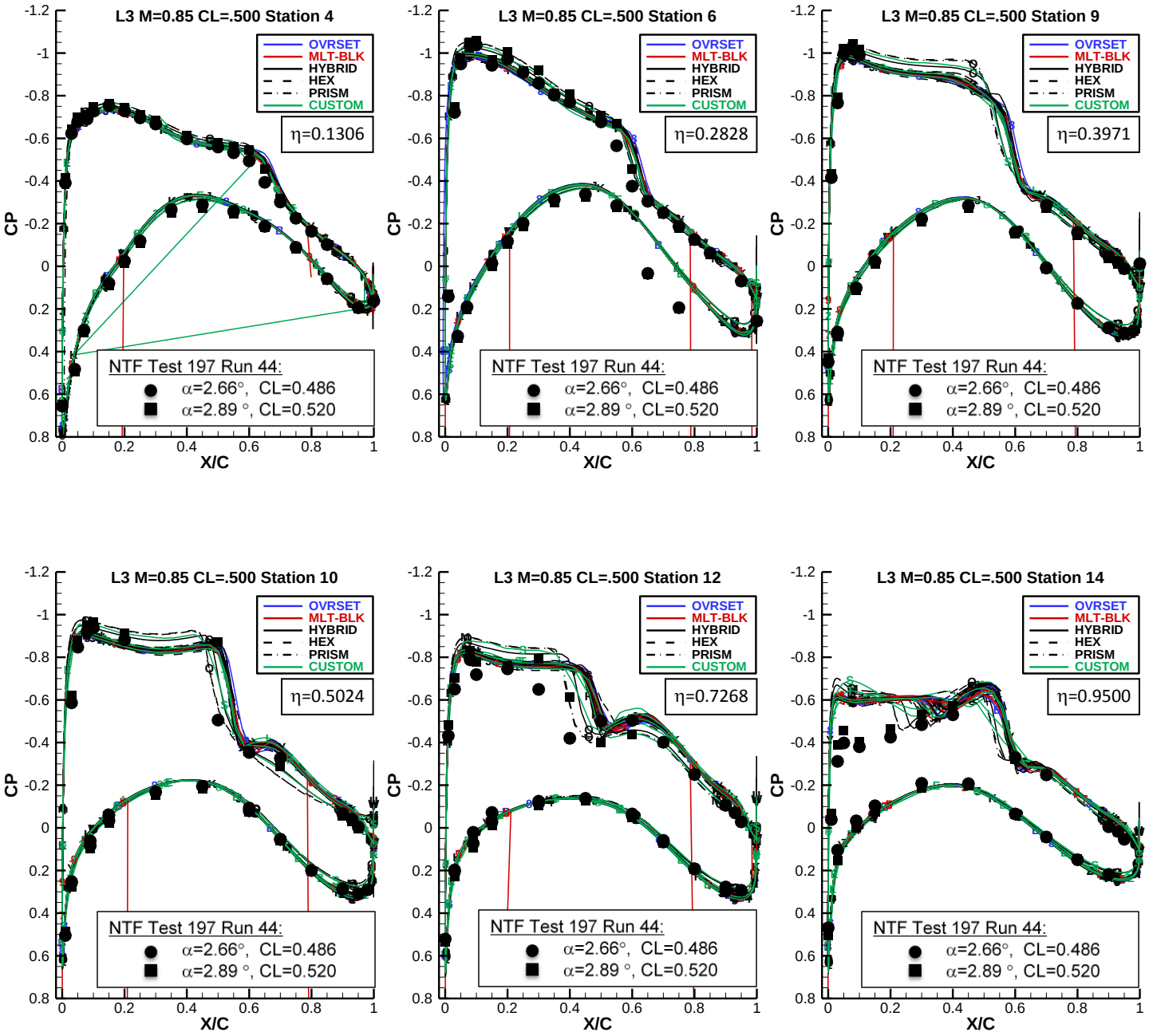


**Figure 13. Case 1 medium grid spanwise variation in wing pressure coefficient.**

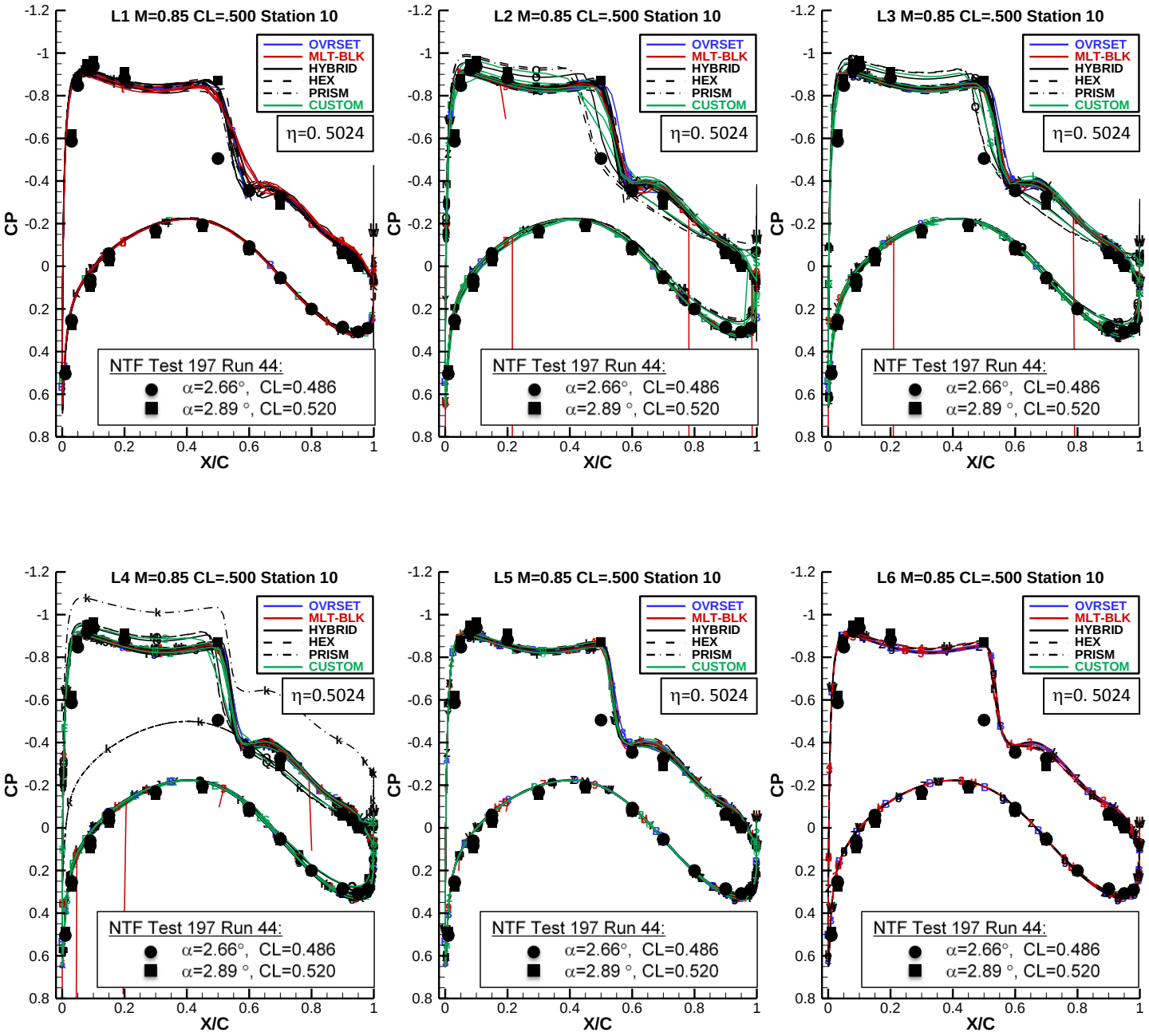


**Figure 14. Case 1 grid refinement trends for wing pressure coefficient at station 10 (η= 0. 5024).**

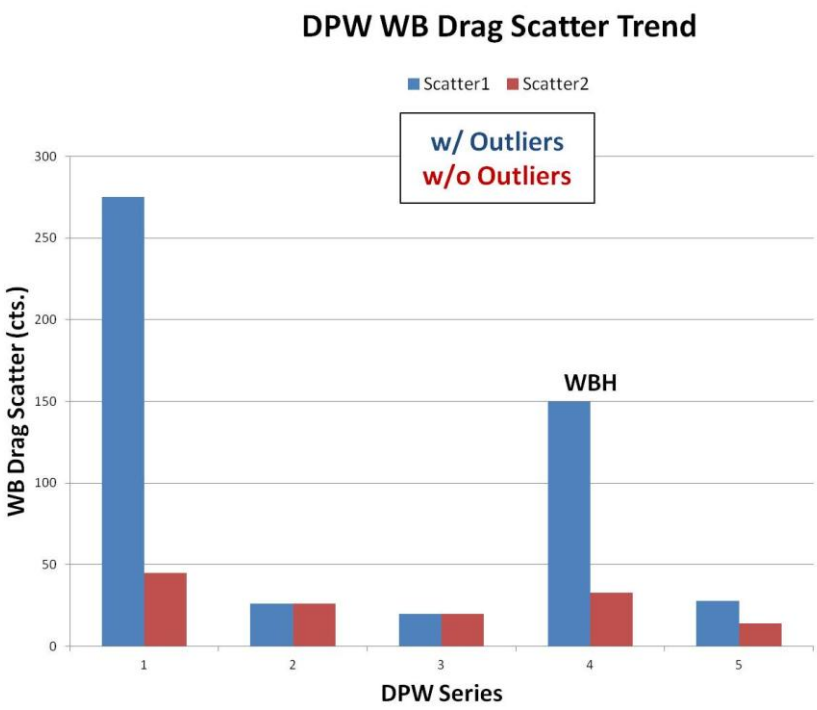


**Figure 15. DPW Series Wing/Body Drag Scatter Trends.**

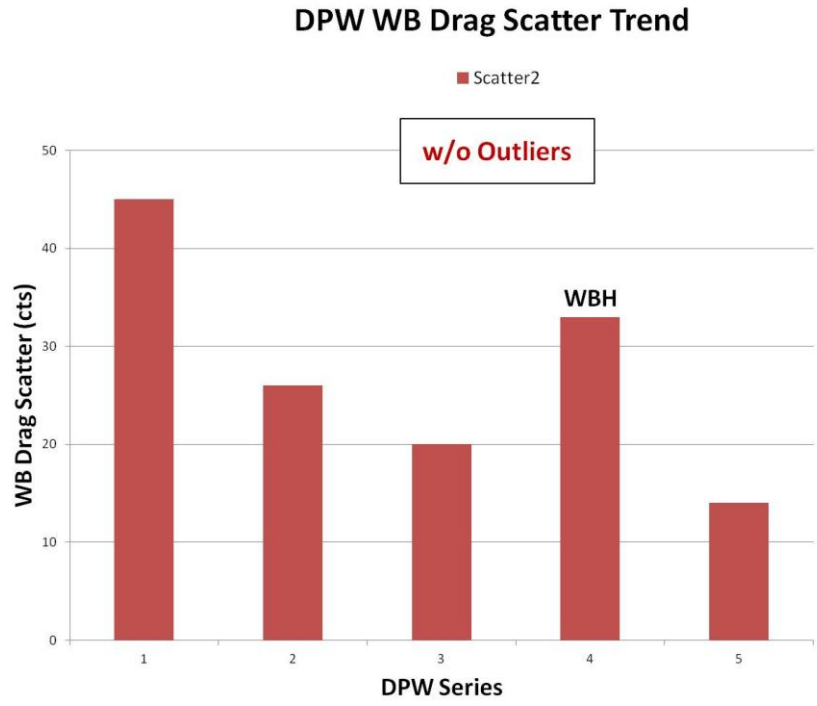


**Figure 16. DPW Series Wing/Body Drag Scatter Trend w/o Outliers.**

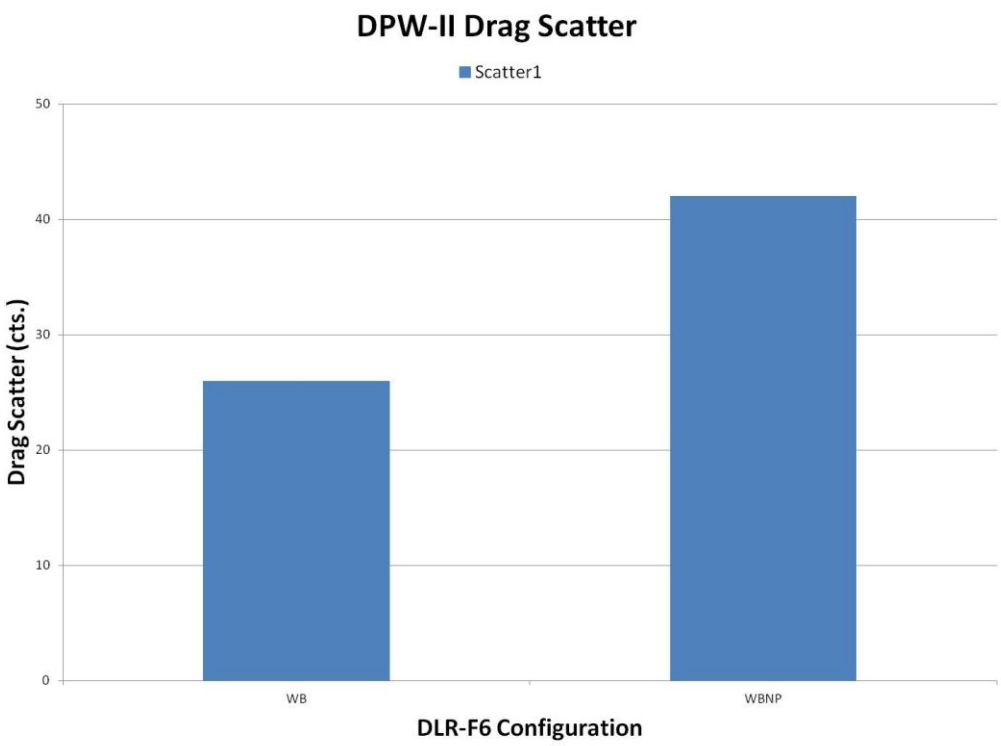


**Figure 17. Effect of Geometric Complexity on Drag Scatter from DPW-II.**

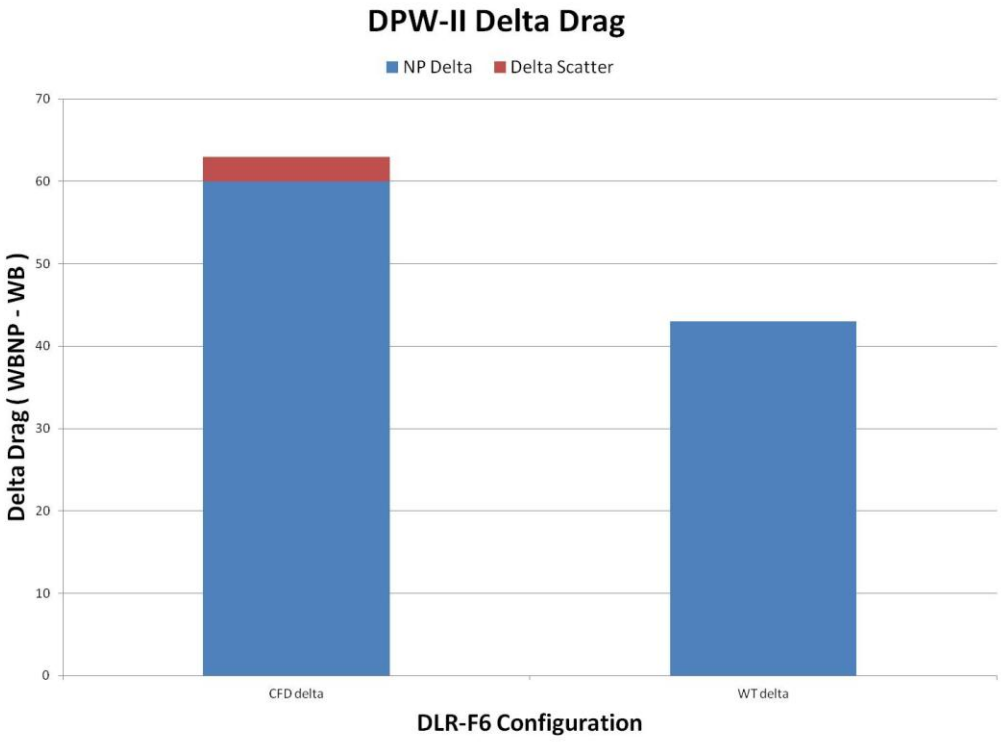


**Figure 18. Comparison of Nacelle/Pylon Drag Deltas between CFD Analyses and WT Experiment.**

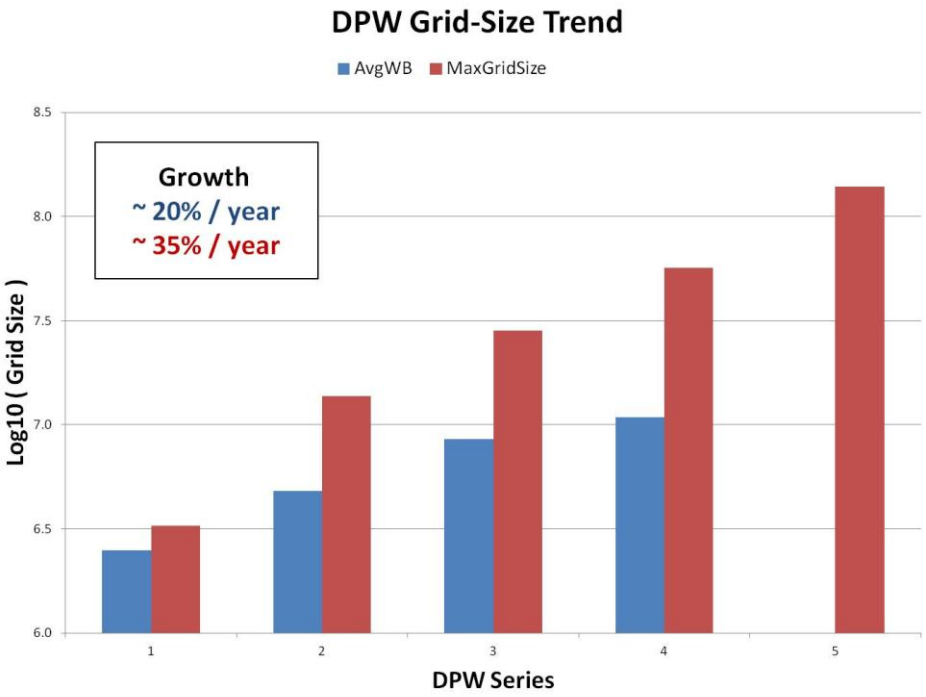


**Figure 19. DPW Series Grid-Size Trends.**